Journal of Inflammation Research

Dovepress
Taylor & Francis Group

Open Access Full Text Article

ORIGINAL RESEARCH

Mechanism Exploration of Dunyeguanxinning in the Treatment of Atherosclerosis Based on UPLC-Q-Orbitrap HRMS Technology, Network Pharmacology, Molecular Docking and Experimental Validation

Dan Wang[1–3], Qipeng Jin[1–3], Jianwei Zhang[4], Xuefei Shi[1–3], Xiaolong Wang[1–3]

[1]Cardiovascular Research Institute of Traditional Chinese Medicine, Shuguang Hospital Affiliated to Shanghai University of Traditional Chinese Medicine, Shanghai, People's Republic of China; [2]Cardiovascular Department of Traditional Chinese Medicine, Shuguang Hospital Affiliated to Shanghai University of Traditional Chinese Medicine, Shanghai, People's Republic of China; [3]Shuguang Hospital Affiliated to Shanghai University of Traditional Chinese Medicine, Branch of National Clinical Research Center for Chinese Medicine Cardiology, Shanghai, People's Republic of China; [4]Department of pharmacy, The NATCM Third Grade Laboratory of Traditional Chinese Medicine Preparations, Shuguang Hospital Affiliated to Shanghai University of Traditional Chinese Medicine, Shanghai, People's Republic of China

Correspondence: Xiaolong Wang, Fax +86 21 51322445, Email wxlqy0214@163.com

Background: Dunyeguanxinning (DYGXN) has been shown to have therapeutic effects in preventing and treating atherosclerosis. However, the active components and anti- atherosclerosis (AS) mechanisms of DYGXN remain to be elucidated.

Purpose: This study aims to explore the functional mechanisms of Dunyeguanxinning (DYGXN) in the prevention and treatment of atherosclerosis (AS).

Methods: The components of DYGXN were identified using UPLC-Q-Orbitrap HRMS technology. Network pharmacology and molecular docking were utilized to explore the functional mechanisms and core targets of DYGXN. An AS mouse model was established to verify the results obtained from network pharmacology.

Results: A total of 20 compounds were identified or tentatively characterized in the DYGXN solution. In total, 149 potential targets of DYGXN and 4,071 AS-related targets were obtained, with 92 overlapping targets between DYGXN and AS. The protein–protein interaction (PPI) network analysis identified 10 key targets, including SRC and STAT3, along with four core subnetworks. Gene ontology (GO) and Kyoto encyclopedia of genes and genomes (KEGG) enrichment analysis indicated that these targets were primarily involved in processes such as phosphorylation, positive regulation of cell migration, inflammatory response and pathways such as lipid and atherosclerosis. Molecular docking demonstrated strong binding affinities between DYGXN compounds and core targets. In vivo experiments showed that DYGXN improved blood lipid levels, reduced pro-inflammatory cytokines, downregulated phosphorylation of Src and STAT3, alleviated hepatic lipid accumulation, and inhibited plaque formation in AS model mice.

Conclusion: DYGXN contains multiple saponins that exert anti-AS effects through the regulation of multiple targets and pathways.

Keywords: Dunyeguanxinning, network pharmacology, atherosclerosis, UPLC-Q-orbitrap HRMS, molecular docking

Introduction

Cardiovascular disease is the leading cause of death and disability worldwide. Over the past 30 years, the number of cardiovascular disease cases has nearly doubled, reaching 523 million, with deaths rising from 12.1 million in 1990 to 19.9 million in 2020 and showing a steady upward trend.[1,2] This number is projected to approach 23.3 million by 2030.[3] Atherosclerosis (AS) is the primary pathological basis and cause of cardiovascular diseases such as stroke, ischemic heart disease, and peripheral vascular disease. Therefore, slowing the progression of AS, stabilizing AS plaques, and reversing the formation of unstable plaques are essential for preventing cardiovascular and cerebrovascular events.[4] Currently,

Received: 16 December 2024
Accepted: 29 March 2025
Published: 9 April 2025

statins are widely used for primary and secondary prevention of atherosclerotic vascular disease due to their cholesterol-lowering effects. However, they can also cause adverse reactions,[5] such as severe myotoxicity, elevated transaminase levels, and intolerance in some patients.[6] Similarly, the antiplatelet agent aspirin is associated with side effects such as gastrointestinal ulcers, increased bleeding risk, and drug resistance.[7,8] Therefore, it is necessary to develop more safe and effective anti-AS drugs to broaden clinical treatment options.

In recent years, patients' preference for "natural" therapies has driven the popularity and development of plant-derived preparations. The genus Dioscorea (family Dioscoreaceae), a group of medicinal and edible homologous plants, have demonstrated significant cardiovascular protective effects. Previous studies have shown that yam (*Dioscorea pseudojaponica*) and its extracts can inhibit inflammation, reduce serum cholesterol, prevent monocyte and smooth muscle cell migration, and decrease AS plaque area.[9,10] *Dioscorea zingiberensis* C. H. Wright is rich in steroidal saponins, which have been shown to possess a wide range of biological activities, including lipid-lowering, anti-myocardial ischemic, anti-inflammatory, and antithrombotic effects, making them highly promising for AS prevention and treatment.[11,12] In China, because of the low cost and significant efficacy of the genus Dioscorea, Dioscorea species extracts have been developed into various cardiovascular pharmaceutical preparations, such as Di'ao Xinxuekang, Dioscornin Tablets, and Dunyeguanxinning (DYGXN). Among these, DYGXN tablets are made from the rhizome of *Dioscorea zingiberensis* and contain water-soluble steroidal saponins as a full-extract tablet. Clinically, DYGXN is primarily used for the treatment of coronary heart disease, angina, hyperlipidemia, and related conditions. Previous studies have shown that the aqueous extract of *Dioscorea zingiberensis* can reduce low-density lipoprotein cholesterol (LDL-C), total cholesterol (TC), triglycerides (TG), and MDA levels in rabbit serum, increase high-density lipoprotein cholesterol (HDL-C) levels, enhance superoxide dismutase (SOD) activity, and decrease plaque area. These findings suggest that the anti-AS effects of water-soluble saponins from *Dioscorea zingiberensis* may be related to lipid regulation, inhibition of oxidative stress, and free radical scavenging.[13] Clinical studies have also confirmed that DYGXN can reduce TC and LDL-C levels, improving AS.[14] DYGXN has been used in China for over 20 years, showing significant efficacy in the treatment of coronary heart disease, angina, hyperlipidemia and AS.[15] However, its specific therapeutic mechanisms remain unclear, especially regarding AS, with limited clinical and basic research available. Further studies are needed to clarify its active components and the underlying mechanisms of anti-AS effects.

Network pharmacology is a novel drug research paradigm developed from bioinformatics, systems biology, pharmacology, and network analysis techniques.[16,17] It enables a comprehensive, integrative, and systematic exploration of the complex biological networks among drugs, targets, and diseases, making it an effective tool for investigating the unknown pharmacological effects of natural products, such as TCM.[18,19] At present, the screening of active components in network pharmacology is often based on databases such as TCMSP, which often lacks accuracy and comprehensiveness. Ultra-high performance liquid chromatography quadrupole orbitrap high resolution mass spectrometry (UPLC-Q-Orbitrap HRMS) provides advantages like high sensitivity, excellent mass accuracy, and good reproducibility, enabling precise qualitative analysis of TCM components and addressing the limitations of TCM chemical databases.[20]

Currently, no studies have applied network pharmacology to investigate the anti-AS effects of DYGXN. Therefore, this study aims to identify the components of DYGXN using UPLC-Q-Orbitrap HRMS to further clarify its active pharmacological basis. Network pharmacology and molecular docking techniques will be used to predict correlations between DYGXN and potential targets, followed by animal experiments to validate relevant targets and pathways. This approach seeks to provide new insights into the anti-AS mechanisms of DYGXN and offer scientific support for its clinical application. The research workflow is presented in Figure 1.

Materials and Methods

Screening the Chemical Components of DYGXN by UPLC-Q-Orbitrap HR-MS

Preparation of the DYGXN Test Solution

Precisely weigh 0.5 g of DYGXN (cat# 14002175065, Jiangsu Huanghe Pharmaceutical Co., Ltd., Jiangsu, China) powder into a 50 mL volumetric flask, add 45 mL of methanol, and ultrasonicate for 75 minutes at room temperature.

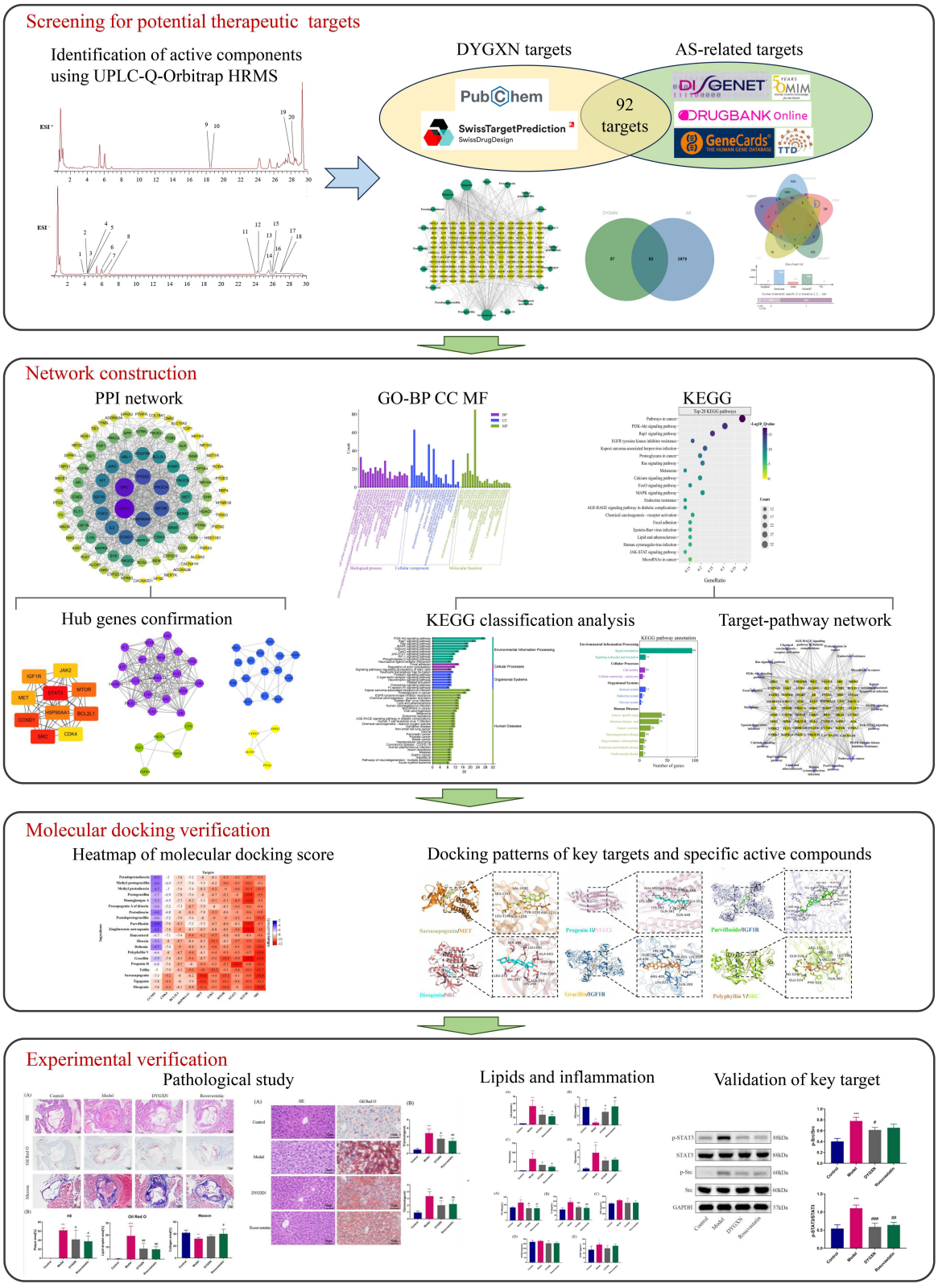

Figure 1 The research workflow of this study.

https://doi.org/10.2147/JIR.S511604

After bringing the solution to volume with methanol, mix thoroughly, then centrifuge at 12,000 rpm for 5 minutes. The supernatant is then diluted 10-fold with 20% methanol to obtain the test solution.

Preparation of the Reference Solution

All reference standards were purchased from Shanghai Tauto Biotech Co., Ltd. Accurately weigh appropriate amounts of the reference standards (≥98% purity)—diosgenin (E-0117), dioscin (E-0098), gracillin (E-0580), protodioscin (E-0163), methyl protodioscin (E-0601), pseudoprotodioscin (E-0897)—into separate 5 mL volumetric flasks, and prepare 0.5 mg/mL methanol solutions of each. Then, transfer suitable volumes of each reference solution and dilute to volume with 20% methanol to obtain a mixed reference solution with a final concentration of approximately 1 μg/mL.

Instrumentation and Conditions

The chemical components of DYGXN were analyzed using the Dionex Ultimate 3000 ultra-high-performance liquid chromatography (UHPLC) system (Thermo Scientific, Waltham, MA, USA) coupled with a Q-Exactive quadrupole-orbitrap high-resolution mass spectrometry (HRMS) (Thermo Fisher Scientific, Waltham, MA, USA). The chromatographic separation was performed using an ACQUITY UPLC® BEH C18 column (2.0 × 100 mm, 1.7 μm, Waters, USA). The mobile phase consisted of methanol (A) and 0.1% formic acid aqueous solution (B), with the following gradient elution program: 0–1 min, 60% A; 1–2 min, 60%–65% A; 2–10 min, 65% A; 10–24 min, 65%–75% A; 24–25 min, 75%–95% A; 25–28 min, 95% A; 28–30 min, 60% A. The flow rate was 0.3 mL/min, the column temperature was 40°C, and the injection volume was 5 μL. The ion source used was an electrospray ionization (ESI) source. Both sheath gas and auxiliary gas were nitrogen, with the auxiliary gas pressure set to 13 arb and the auxiliary heater temperature at 350°C. The ion transfer tube temperature was 320°C, with an automatic gain control (AGC) of 1×10^6 and an S-lens RF level of 50. The sheath gas pressure for both positive and negative ion modes was set to 35 arb, and the spray voltages were 3.5 kV for positive ion mode and 2.5 kV for negative ion mode. The scanning mode was full scan for both positive and negative ions, with a scan range of m/z 100–1500, including one full scan at a resolution of 70,000 FWHM in the first stage and one full scan at a resolution of 17,500 FWHM in the second stage. The collision energy gradients were set to 10V, 20V, and 40V.

Compound Identification

The study identified compounds by consulting relevant literature and utilizing the PubChem compound database and Thermo Xcalibur software (version 2.2, Thermo Fisher Scientific, USA). Compound names, molecular formulas, exact relative masses, and accurate mass-to-charge ratios (m/z) were compiled for four ionization modes: $[M+H]^+$, $[M-H]^-$, $[M-HCOO]^-$, and $[M+Na]^+$, building a custom compound database. Data analysis was conducted by referencing the peak time of the reference compounds along with existing literature reports.

Network Pharmacology Study

Prediction and Screening of Anti-AS Targets of DYGXN

The identified chemical constituents were used to obtain their 3D structures from the PubChem database, and their potential targets were assessed and predicted using the SwissTargetPrediction database[21] (http://www.swisstargetprediction.ch/). Using "atherosclerosis" as a keyword, anti-AS targets were identified by querying GeneCards[22] (https://www.genecards.org/), OMIM[23] (https://omim.org/), TTD[24] (https://db.idrblab.net/ttd/), DrugBank[25] (https://go.drugbank.com/), and DisGeNET[26] (https://disgenet.com/) database with "homo sapiens" as the species filter. All disease targets and the predicted targets of drug component were standardized to gene symbols.

Construction of the "Component-Target" Network for DYGXN

The drug and disease targets obtained were used to generate a Venn diagram on the jvenn website (https://jvenn.toulouse.inrae.fr/app/example.html) to identify common targets between DYGXN and AS. The active components and common targets were then imported along with their network and type text files into Cytoscape 3.7.2 software to construct the "component-target" network.

Construction of the Protein–Protein Interaction (PPI) Network and the Screening of Core Targets

The identified common targets were input into the STRING database[27] (https://string-db.org/) to construct the PPI network, with the protein species set to "homo sapiens" and confidence level adjusted to the highest (score > 0.9), while hiding unconnected nodes within the network. The resulting PPI network was visualized using Cytoscape 3.7.2. Clustering and topological analyses were performed using the CytoHubba and MCODE plugins within the software, enabling the identification of core targets and potential protein functional modules related to DYGXN's anti- AS effects.

Gene Ontology (GO) and Kyoto Encyclopedia of Genes and Genomes (KEGG) Enrichment Analysis

The DAVID database[28] (https://david.ncifcrf.gov/) was used to conduct KEGG pathway analysis and GO enrichment analysis for core targets. The bioinformatics platforms ChiPlot (https://www.chiplot.online/) and Bioinformatics[29] (http://www.bioinformatics.com.cn/) were utilized to create bubble plots and enrichment classification diagrams.

Construction of the "Target–Pathway" Network

The identified anti-AS targets and the top 20 KEGG pathway enrichment results were imported into Cytoscape 3.7.2 software to construct a "target–pathway" network. Node color and size were adjusted based on degree values.

Molecular Docking Verification

Molecular docking was performed between 10 selected core targets and 20 identified compounds. The 3D structure (SDF format) of the 20 compounds was downloaded from the PubChem database. For compounds without an SDF file, SMILE structures were collected, and 3D structures were predicted using RDKit. SDF files were then converted to PDB format in OpenBabel, and each compound was processed with the prepare_ligand command to add hydrogen and charges, resulting in PDBQT files. The 10 target proteins served as receptors. PDB files for each protein were retrieved from the UniProt database, and water molecules and sulfate ions were removed using PyMOL. Receptor preparation involved adding hydrogen and charges with the prepare_receptor4 command, followed by exporting to PDBQT format. Protein pocket parameters containing protein residues were acquired in AutoDock Tools, and each set of protein pocket parameters, along with three AutoDock Vina parameters (energy_range = 5, exhaustiveness = 8, num_modes = 8), were saved as a "config.txt" file. Autodock Vina was run by Lamarckian genetic algorithm in the cmd command mode of the system to dock compound ligands with the protein pockets, and docking scores were recorded. PyMOL 3.0.0 was used to analyze the results and generate visual representations.

Animal Experiments

Animals

Ten six-week-old SPF-grade C57BL/6J male mice and thirty male Apolipoprotein E knocked out ($ApoE^{-/-}$) mice (C57BL/6J background), weighing approximately 18–24g, were purchased from Beijing Weitonglihua Experimental Animal Technology Co., Ltd. (Beijing, China).The mice were housed for one week of acclimation at the Experimental Animal Center of Shanghai University of Traditional Chinese Medicine under a controlled temperature of 26°C and a 12-hour light/dark cycle, with free access to food and water. All animal experiments were conducted in accordance with the Laboratory Animal-Guideline for Ethical Review of Animal Welfare (GB/T 35892–2018) and were approved by the Ethics Committee of Shanghai University of Traditional Chinese Medicine (ethics approval number: PZSHUTCM220627030).

Grouping, Modeling, and Administration

Ten C57BL/6J mice were designated as the control group. The $ApoE^{-/-}$ mice were randomly divided into three groups: model group, DYGXN group, and rosuvastatin group, with ten mice in each group, housed separately. After a one-week acclimation period, all groups except the control group were fed a high-fat diet (composition: 78.8% breeding feed, 1% cholesterol, 0.2% bile salts, 10% lard, and 10% egg yolk powder). In addition to the high-fat diet, the DYGXN group received DYGXN (cat# 14002175065, Jiangsu Huanghe Pharmaceutical Co., Ltd., Jiangsu, China) at a dose of 146 mg/kg/day via gavage. The rosuvastatin group received rosuvastatin (cat# 132756, AstraZeneca Pharmaceuticals (China) Co., Ltd) at an equivalent dose of 2.08 mg/kg/day via gavage (The drug dosage is calculated based on the equivalent dose between human and mice), while the control and model groups were given an equal volume of purified water daily. Mice

were weighed weekly at the same time, and after 12 weeks of feeding, blood was collected from the eyes, and samples of the heart, liver, and aorta were obtained for analysis.

Histopathological Staining of the Aortic Roots and Liver Tissue in Mice

The mouse heart and liver were fixed in 4% paraformaldehyde, embedded in OTC, and sectioned into frozen slices with a thickness of 6 μm, ensuring that all three aortic root valves appeared in a single section. According to the manufacturer's instructions, the Hematoxylin and eosin (HE) staining was performed to assess plaque area and liver damage, Oil Red O staining was used to evaluate plaque and hepatic lipid accumulation, and Masson staining was used to assess plaque stability. Image-Pro Plus 6.0 (Media Cybernetics, USA) was utilized for analysis.

Biochemical Analysis of Mouse Plasma and Liver

After anesthetizing the mice, blood samples were collected from the orbital venous plexus. The blood was allowed to stand for 2 hours, then centrifuged at 4°C and 4000 rpm for 15 minutes. Serum was collected and stored at −80°C. According to the kit instructions, serum levels of HDL-C (cat# A112-1-1), LDL-C (cat# A113-1-1), TC (cat# A111-1-1), and TG (cat# A110-1-1) were measured, along with hepatic cholesterol and triglyceride levels. All assay kits were purchased from the Nanjing Jiancheng Bioengineering Institute (Nanjing, China).

Enzyme-Linked Immunosorbent Assay (ELISA) for Inflammatory Cytokines

Serum levels of nuclear factor kappa B (NF-κB) (cat# H202-1-2), interleukin 6 (IL-6) (cat# H007-1-2), tumor necrosis factor alpha (TNF-α) (cat# H052-1-2), vascular cellular adhesion molecule-1(VCAM-1) (cat# H066-1-2), intercellular adhesion molecule-1 (ICAM-1) (cat# H065-1-2), and interleukin 1 beta (IL-1β) (cat# H002-1-1) were measured according to the manufacturer's instructions for each ELISA kit. All kits were purchased from the Nanjing Jiancheng Bioengineering Institute (Nanjing, China).

Western Blot Analysis

Aorta proteins were extracted using RIPA with PMSF, and protein concentration was measured using a BCA protein assay kit. Protein samples were separated by 10% sodium dodecyl sulfate–polyacrylamide gel electrophoresis and transferred onto PVDF membranes. The membranes were blocked with blocking solution at 37°C for 2 hours, then incubated overnight at 4°C with primary antibodies: Src (cat# 2109, 1:1000, Cell Signaling Technology), p-Src (cat# 6943, 1:1000, Cell Signaling Technology), STAT3 (cat# A19566, 1:1000, ABclonal Technology), p-STAT3 (cat# 9145, 1:2000, Cell Signaling Technology), and GAPDH (cat# 2118, 1:5000, Cell Signaling Technology). After three washes in TBST (5 min each), membranes were incubated for 1 hour at room temperature with HRP-conjugated goat anti-rabbit /mouse IgG (1:5000). Following three more washes in TBST, bands were visualized using chemiluminescent reagents, and band intensity was quantitatively analyzed using ChemiScope Capture image analysis software (Shanghai Qinxiang Scientific Instruments Co., Ltd., China).

Statistical Analysis

All data are presented as mean±SD. One-way analysis of variance (ANOVA) was employed for comparisons between multiple groups, with a significance level set at $P < 0.05$. GraphPad Prism 7.00 was used for data visualization.

Results

Identification of Original Chemical Components in DYGXN

The mixed reference solution and DYGXN test solution were analyzed by UPLC-Q-Orbitrap HRMS under the chromatographic conditions described in "2.1.3" and the mass spectrometry conditions in "2.1.4". Total ion chromatograms were obtained in both positive and negative ion modes, as shown in Figure 2. In total, 20 compounds were identified or tentatively characterized in the DYGXN solution, among which 6 compounds were confirmed by comparison with reference standards. This study provides a scientific basis for the quality control, clinical application, pharmacokinetics, and pharmacodynamic foundation of DYGXN. Identification results are summarized in Table 1.

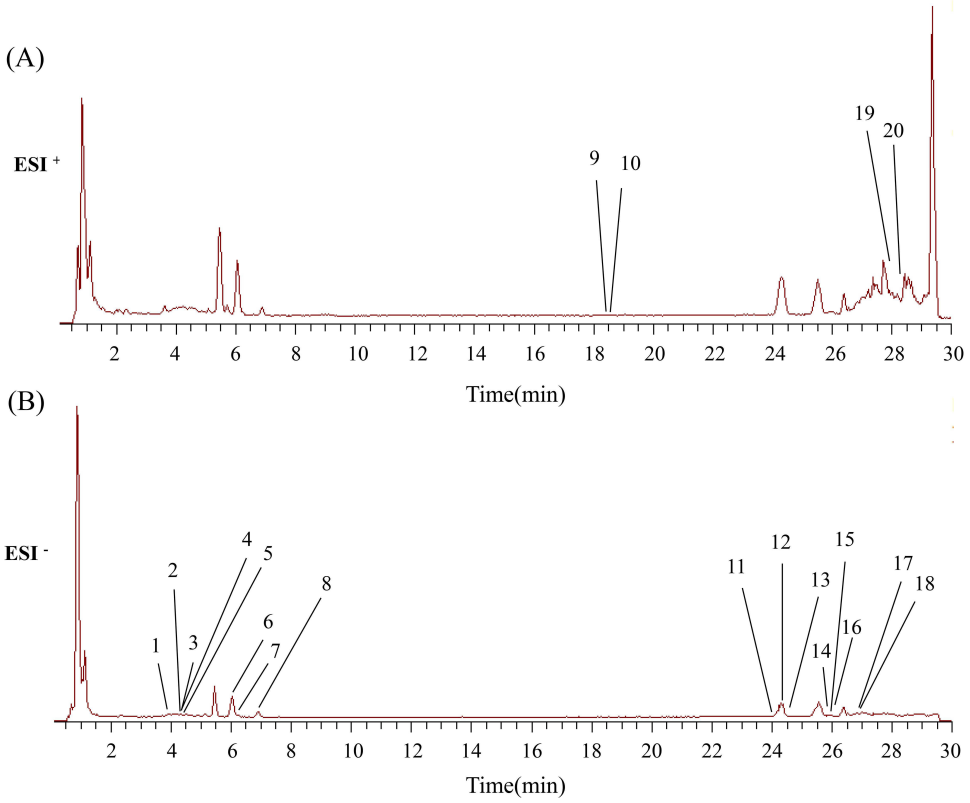

Figure 2 Identification of components in DYGXN. (**A**)Total ion chromatogram of DYGXN test solution in positive ion mode. (**B**) Total ion chromatogram of DYGXN test solution in negative ion mode.

Network Pharmacology Analysis Results

DYGXN Components and Targets

A total of 149 target proteins were predicted for 20 DYGXN components by using SwissTargetPrediction. A component-target network of DYGXN was constructed using Cytoscape 3.7.2, where green circles represent DYGXN components and yellow circles represent target genes; the larger the node, the higher the number of targets. The top three components

Table 1 Chemical Components of DYGXN

No.	Compounds	Retention Time (min)	Ion Mode	Theoretical Mass (m/z)	Measured Mass (m/z)	Error (ppm)	Molecular Formula	Peak Area (10^7)
1	Parvifloside	3.9	$[M\text{-}HCO2]^-$	1271.5903	1271.5916	1.009	$C_{57}H_{94}O_{28}$	4.75
2	Protogracillin	4.34	$[M\text{-}HCO2]^-$	1109.5374	1109.5388	1.24	$C_{51}H_{84}O_{23}$	10.17
3	Protodioscin*	4.34	$[M\text{-}HCO2]^-$	1093.5425	1093.5396	−2.725	$C_{51}H_{84}O_{22}$	2.90
4	Methyl protogracillin	4.34	$[M\text{-}HCO2]^-$	1123.5531	1123.5543	1.091	$C_{52}H_{86}O_{23}$	9.97
5	Methyl protodioscin*	4.49	$[M\text{-}HCO2]^-$	1107.5582	1107.5635	4.786	$C_{52}H_{86}O_{22}$	0.93
6	Huangjiangsu A	6.05	$[M\text{-}HCO2]^-$	1091.5269	1091.5278	0.871	$C_{51}H_{82}O_{22}$	51.62
7	Pseudoprotodioscin*	6.23	$[M\text{-}HCO2]^-$	1075.5320	1075.5333	1.269	$C_{51}H_{82}O_{21}$	6.14
8	Pseudoprotogracillin	6.81	$[M\text{-}HCO2]^-$	1091.5269	1091.5286	1.54	$C_{51}H_{82}O_{22}$	0.11
9	Tigogenin	18.47	$[M+Na]^+$	439.3183	439.3181	−0.333	$C_{27}H_{44}O_3$	0.03
10	Sarsasapogenin	18.58	$[M+Na]^+$	439.3183	439.318	−0.561	$C_{27}H_{44}O_3$	0.02
11	Polyphyllin V	24.06	$[M\text{-}HCO2]^-$	767.4212	767.4224	1.547	$C_{39}H_{62}O_{12}$	0.41
12	Zingiberensis newsaponin	24.32	$[M\text{-}HCO2]^-$	1091.5269	1091.528	0.981	$C_{51}H_{82}O_{22}$	52.51
13	Deltonin	24.53	$[M\text{-}HCO2]^-$	929.4741	929.4739	−0.19	$C_{45}H_{72}O_{17}$	0.04

(*Continued*)

https://doi.org/10.2147/JIR.S511604

Table 1 (Continued).

No.	Compounds	Retention Time (min)	Ion Mode	Theoretical Mass (m/z)	Measured Mass (m/z)	Error (ppm)	Molecular Formula	Peak Area (10^7)
14	Prosapogenin A of dioscin	25.83	$[M\text{-}HCO2]^-$	767.4212	767.4244	4.101	$C_{39}H_{62}O_{12}$	0.02
15	Dioscin*	25.94	$[M\text{-}HCO2]^-$	913.4791	913.4812	2.253	$C_{45}H_{72}O_{16}$	10.79
16	Gracillin*	26.13	$[M\text{-}HCO2]^-$	929.4741	929.4774	3.554	$C_{45}H_{72}O_{17}$	0.25
17	Progenin II	26.91	$[M\text{-}HCO2]^-$	767.4212	767.4239	3.462	$C_{39}H_{62}O_{12}$	0.14
18	Trillin	26.99	$[M\text{-}HCO2]^-$	621.3633	621.3649	2.488	$C_{33}H_{52}O_8$	0.67
19	Diosgenin*	28.07	$[M+H]^+$	415.3207	415.3204	−0.582	$C_{27}H_{42}O_3$	3.11
20	Daucosterol	28.4	$[M+Na]^+$	599.4282	599.4276	−1.002	$C_{35}H_{60}O_6$	0.38

Note: *Indicates the component was authenticated using reference standards.

with the highest degree values were diosgenin, sarsasapogenin, and tigogenin, each interacting with 72, 75, and 75 targets, respectively (Figure 3A; specific targets listed in Supplemental Table 1).

Screening of AS Targets

A total of 5,739 AS-related targets were obtained from GeneCards, with 2,889 potential targets selected based on a relevance score of ≥ 0.757847. Additionally, anti-AS targets were identified using OMIM, TTD, DrugBank, and DisGeNET databases, yielding 525, 36, 37, and 2,044 targets, respectively. After removing 1,460 duplicate targets, a total of 4,071 AS-related targets were obtained (Figure 3B; detailed targets are listed in Supplemental Table 2).

PPI Network Construction

A total of 92 intersecting targets between DYGXN and AS were obtained from the jvenn website and a Venn diagram was generated (Figure 4A, Supplemental Table 3). These 92 targets were imported into the String database, and the resulting PPI network was visualized in Cytoscape software, with the topological features of all nodes calculated. After

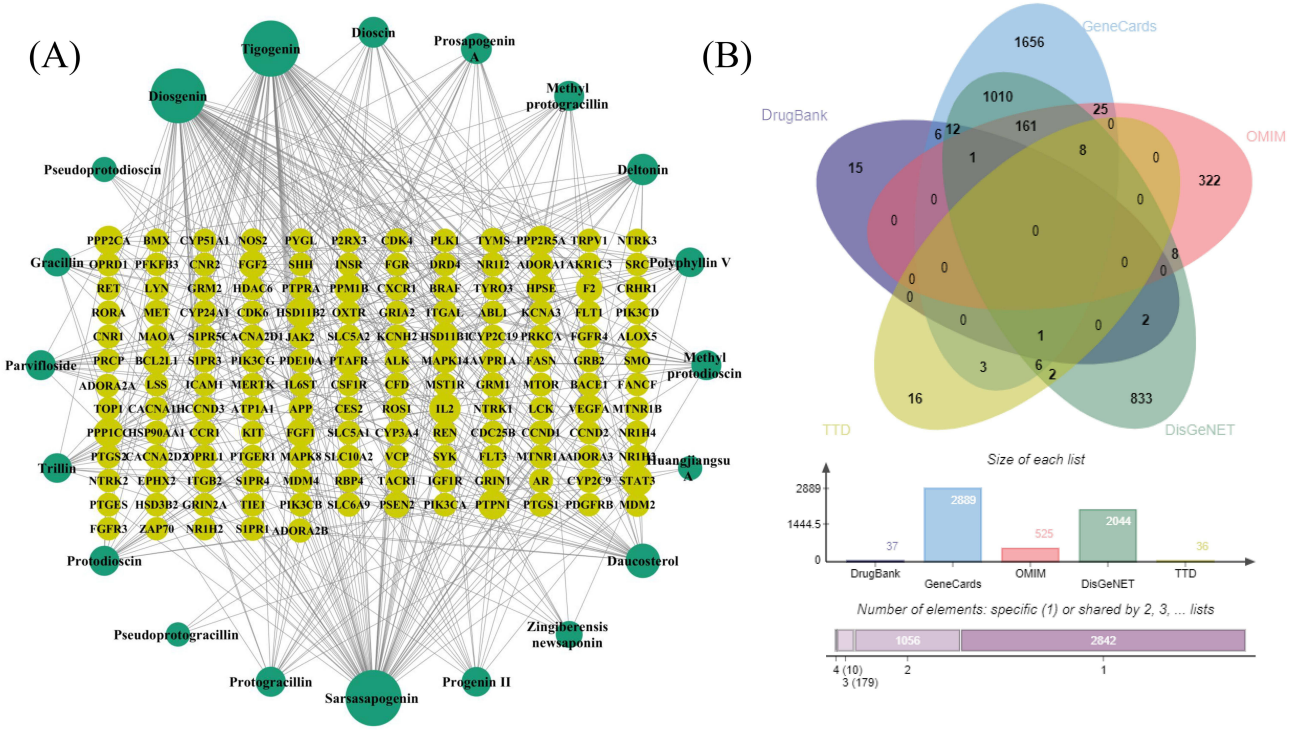

Figure 3 (**A**) DYGXN compound-target network; (**B**) Venn diagram of AS-related targets from five databases.

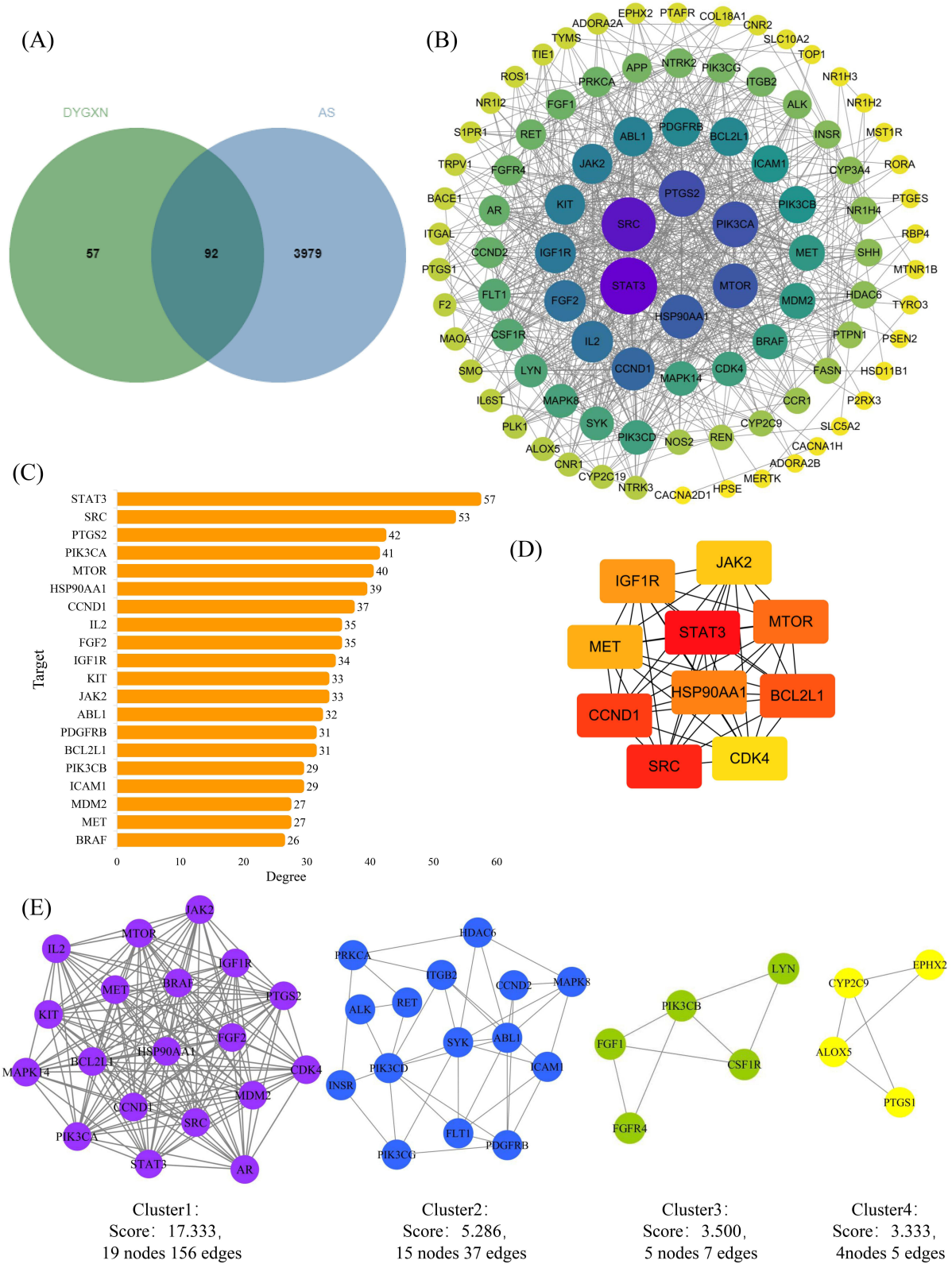

Figure 4 (**A**) The Venn diagram of DYGXN treatment targets for AS: A total of 92 intersecting targets between DYGXN and AS were obtained. (**B**) PPI network diagram: Darker colors and larger node sizes represent higher degree values. (**C**) Bar chart of the top 10 targets based on degree values. (**D**) Ten core target genes selected by the CytoHubba plugin. (**E**) Four sub-networks obtained from protein clustering of targets using the MCODE plugin.

https://doi.org/10.2147/JIR.S511604

removing nodes that were disconnected and had fewer edges in the PPI network, a final network was presented with 92 targets and 744 edges. Supplemental Table 4 shows the specific topology parameters. As shown in Figure 4B, nodes with darker colors and larger areas correspond to higher degree values, suggesting they may be key targets for DYGXN in treating AS. A bar chart was created for the top 10 targets based on degree values (Figure 4C). Using the CytoHubba plugin, 10 core target genes were identified: STAT3, SRC, MTOR, IGF1R, MET, CDK4, BCL2L1, JAK2, HSP90AA1, and CCND1 (Figure 4D). The MCODE plugin was then used for protein clustering, resulting in four sub-networks based on Degree Cutoff ≥ 2, Nude Score Cutoff ≥ 0.2, and K-Core ≥ 2 (Figure 4E). These four networks were further analyzed using biological process (BP) analysis. Cluster 1 was involved in 152 biological processes such as phosphorylation, positive regulation of vascular-associated smooth muscle cell proliferation, signal transduction, and response to xenobiotic stimulus. Cluster 2 was involved in 80 processes like phosphorylation, cell surface receptor protein tyrosine kinase signaling pathway, peptidyl-tyrosine phosphorylation, positive regulation of kinase activity, and positive regulation of endothelial cell migration. Cluster 3 was involved in 21 biological processes, including cell surface receptor protein tyrosine kinase signaling pathway and positive regulation of cell population proliferation. Cluster 4 was associated with the long-chain fatty acid biosynthetic process (Supplementary Materials).

GO and KEGG Functional Enrichment Analysis

GO and KEGG functional enrichment analysis was performed on the 92 targets, yielding 83 molecular functions (MF), 443 biological processes (BP), 57 cellular components (CC), and 141 signaling pathways. Figure 5A lists the top 20 BP, MF, and CC terms ($P < 0.01$). The findings indicate that the potential targets of DYGXN in AS treatment are associated with molecular functions such as transmembrane receptor protein tyrosine kinase activity, protein tyrosine kinase activity, ATP binding, enzyme binding, kinase activity, and protein binding. These targets are involved in biological processes including phosphorylation, cell surface receptor protein tyrosine kinase signaling pathway, positive regulation of kinase activity, multicellular organism development, negative regulation of apoptotic process, positive regulation of cell migration, angiogenesis, cell migration, and inflammatory response. Additionally, they are related to cellular components such as receptor complex, plasma membrane, membrane raft, axon, and cell surface. Figure 5B lists the top 20 KEGG signaling pathways. After removing irrelevant broad-spectrum pathways, KEGG enrichment analysis shows that DYGXN's potential mechanisms in AS treatment primarily involve pathways such as Rap1 signaling pathway, focal adhesion, lipid and atherosclerosis, and the JAK-STAT signaling pathway. We hypothesize that DYGXN may improve AS by regulating phosphorylation, cell migration, inflammatory response, and lipid metabolism. Figure 5C and D illustrate the secondary classification of KEGG pathways, categorized into four main areas: environmental information processing (signal transduction, signal molecules, and interaction), cellular processes (cell motility, cellular community), organismal systems (immune, endocrine, and nervous systems), and human diseases (specific types of cancer, infectious diseases: viral, cancer overview, neurodegenerative diseases, drug resistance: antineoplastic, endocrine and metabolic diseases, cardiovascular diseases). Figure 6 displays the top 20 signaling pathways along with their corresponding target genes. Among these, the lipid and atherosclerosis pathway is particularly significant, comprising 14 target genes, including SRC and STAT3. Given that SRC and STAT3 have the highest degree values in the PPI network and demonstrate strong binding affinity with DYGXN active compounds, they likely serve as key targets in DYGXN's anti-AS effects. Therefore, we selected the Src/STAT3 pathway for further experimental validation.

Molecular Docking Results

Molecular docking was used to validate the binding affinity between the screened compounds and core targets. A binding energy ≤ −5 kcal/mol indicates a good affinity with the key targets, and a score < −7 kcal/mol is considered to indicate a strong binding affinity.[30] The binding affinity results heatmap are shown in Figure 7. SRC, STAT3, IGF1R, MTOR, JAK2, and MET exhibited low binding energies, suggesting strong docking activity and stability between these proteins and the active compounds. These proteins may represent potential targets through which DYGXN exerts its therapeutic effects. The interactions between the representative target proteins and active compounds are primarily driven by Van der Waals forces and hydrogen bonds. Figure 8 illustrates six representative "target proteins-active compounds" docking patterns.

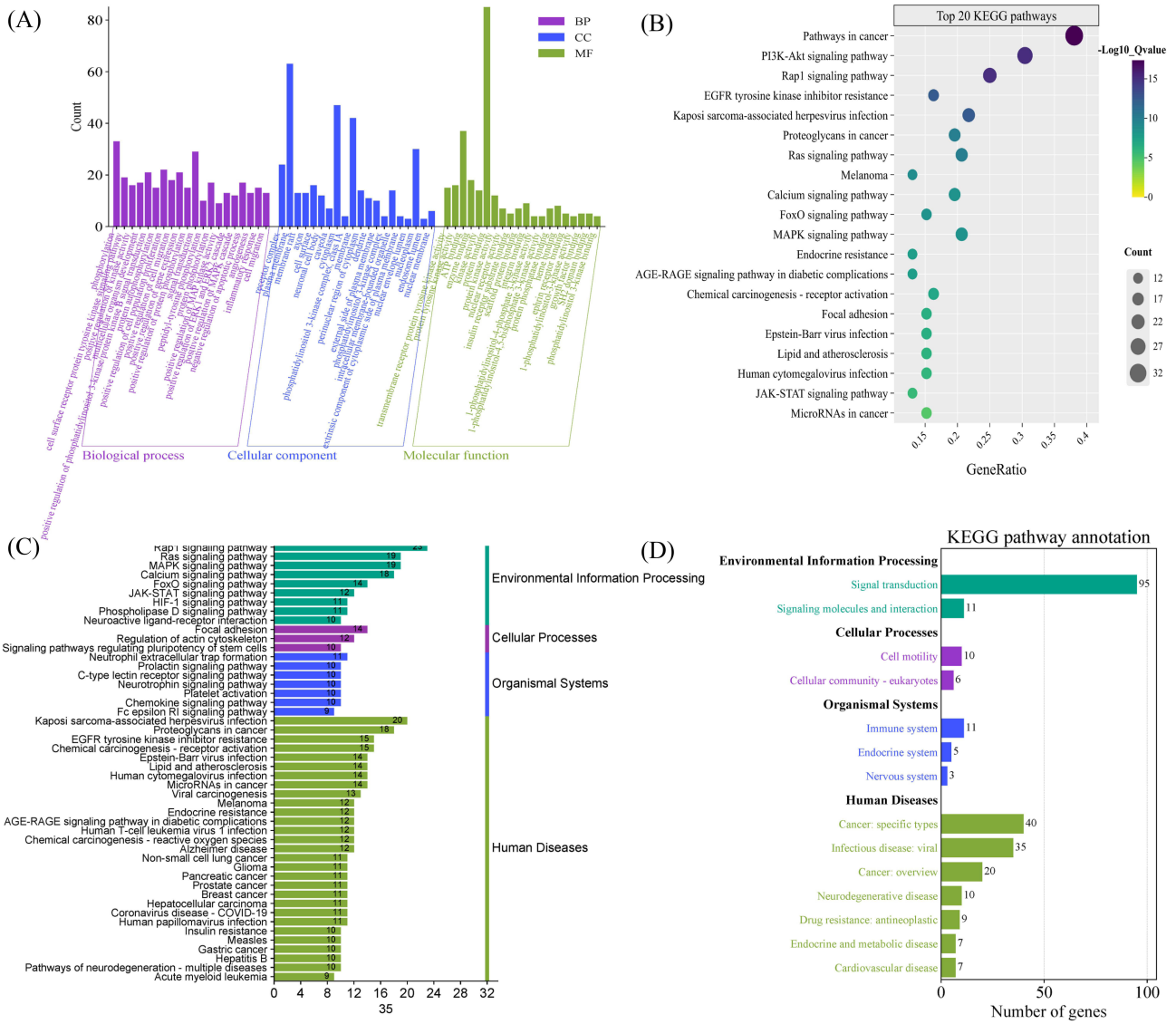

Figure 5 (**A**) Top 20 GO enrichment analysis results. Purple represents biological processes (BP), blue represents cellular components (CC), and green represents molecular functions (MF). (**B**) Top 20 enriched KEGG signaling pathways, with larger circles representing a greater number of enriched genes and deeper colors indicating smaller p-values. (**C** and **D**) display KEGG classification analysis for the top 50 pathways based on KEGG taxonomic analysis.

Effect of DYGXN on the Formation of AS

Effect of DYGXN on Aortic Root Plaque Formation in Mice

HE staining results showed that the aortic roots in the control group mice exhibited smooth intima and intact structure. In contrast, the model group mice developed large and prominent atherosclerotic plaques ($P < 0.001$). Plaques were protruding into the lumen, narrowing the vessel, with foam cell infiltration forming a lipid core. A significant amount of inflammatory cell infiltration was observed, with a thinning and uneven fibrous cap, and the media, composed of smooth muscle cells, was thinned. Cholesterol crystals and calcified foci were visible in some plaques. After treatment with DYGXN, the plaque area decreased ($P < 0.05$). Oil Red O staining showed that there were almost no red lipid deposits in aortic root of the control group, while large areas of red lipid deposits were visible in aortic roots of the model group ($P < 0.0001$). DYGXN treatment reduced the red lipid deposition ($P < 0.01$). Masson staining results showed that the intima of the aortic roots in the control group was smooth, flat, and continuous, with neatly arranged collagen fibers. In contrast, the model group exhibited disorganized collagen fibers with lighter-colored plaques, a thinner fibrous cap ($P < 0.01$), and increased instability of the plaque. After DYGXN treatment, collagen fibers were more organized, and the

https://doi.org/10.2147/JIR.S511604

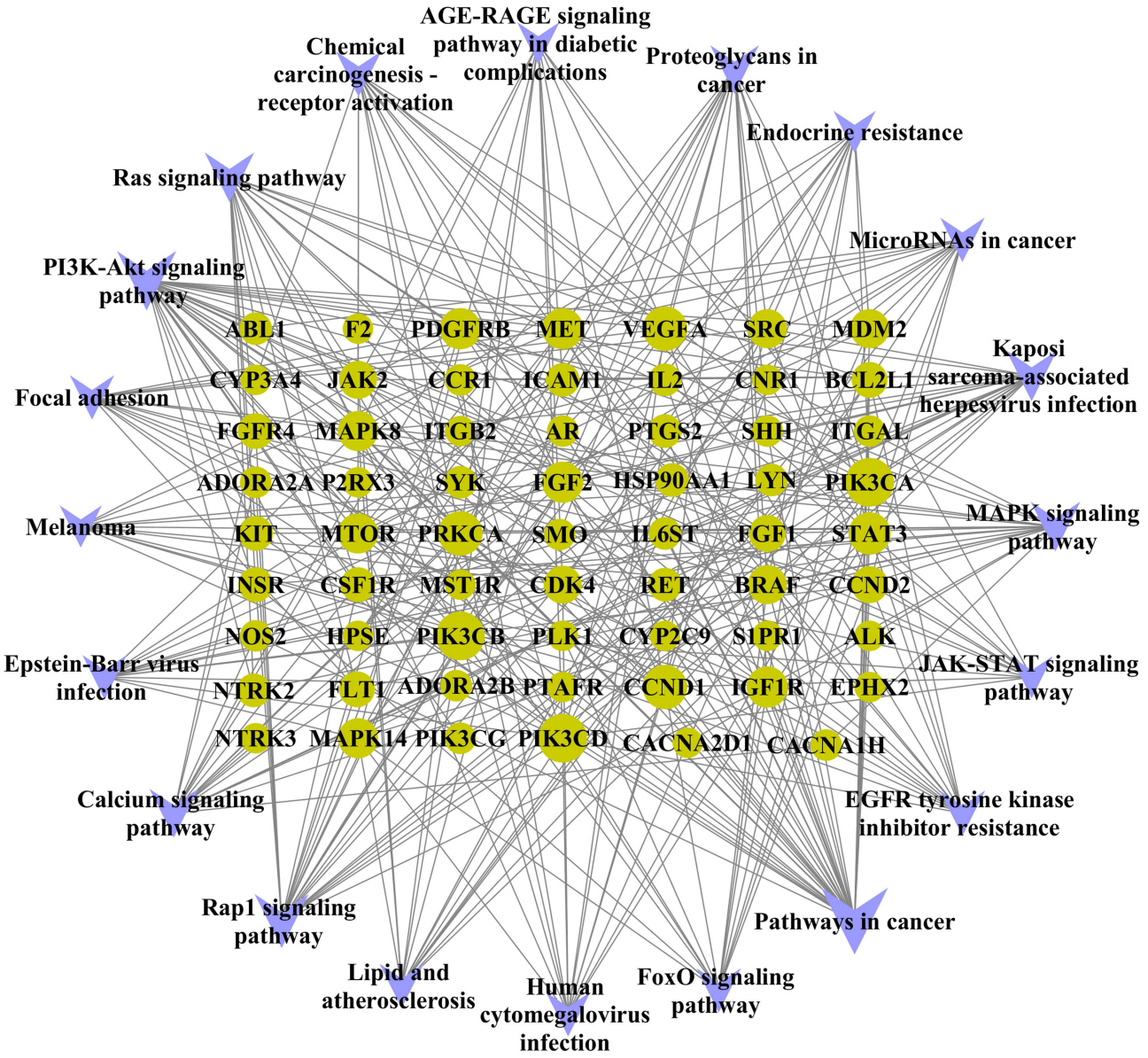

Figure 6 Correspondence between the top 20 signaling pathways and target genes: purple arrows represent pathways, and yellow circles represent genes within those pathways.

blue-stained collagen fibers increased, indicating enhanced plaque stability, although no statistically significant differences were observed between the DYGXN group and the Model group (Figure 9).

Effects of DYGXN on Liver Histomorphology and Lipid Accumulation

HE staining showed that liver cells in the control group had intact structure, clear borders, and visible nuclei, with well-preserved liver lobule structure. In contrast, the model group exhibited abnormal liver lobule structure, with blurred borders, loose arrangement of hepatocytes, and numerous fat vacuoles of varying sizes within the cells. The structures of hepatic sinusoids and hepatic cords were unclear. In the DYGXN and rosuvastatin groups, fewer fat vacuoles were observed. Oil Red O staining revealed that the control group had minimal red lipid droplet deposition, whereas the model group showed large and deep red lipid droplet areas in the liver. In contrast, DYGXN and rosuvastatin groups exhibited less lipid accumulation in the liver. Compared to the control group, the model group showed significantly elevated liver TG and TC levels ($P < 0.001$), as shown in Figure 10A, while DYGXN treatment alleviated the accumulation of liver TC and TG ($P < 0.05$, $P < 0.01$) (Figure 10B).

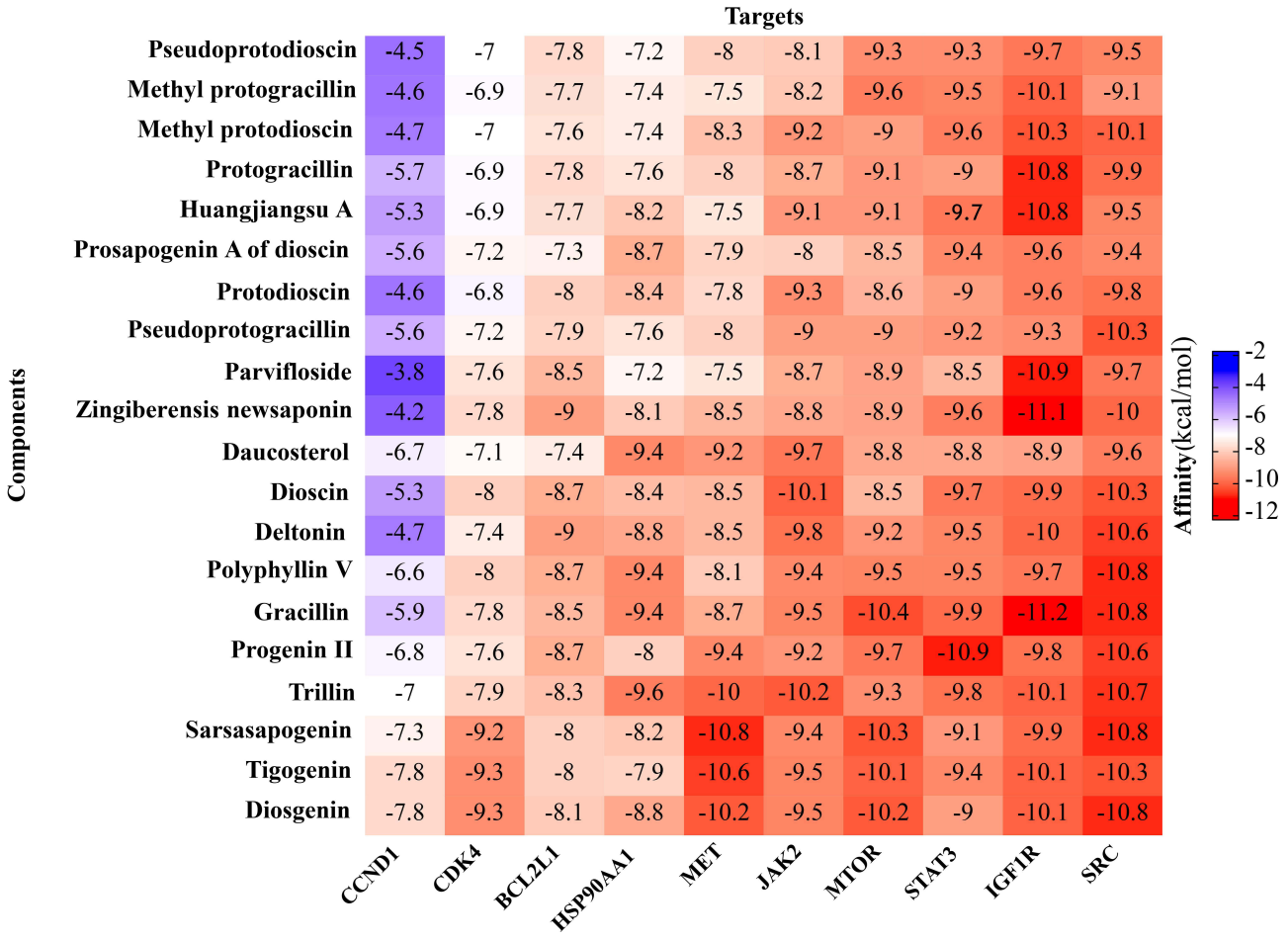

Figure 7 Heatmap of molecular docking binding energies. The vertical axis represents the 20 chemical compounds, while the horizontal axis represents the 10 core targets. Darker colors indicate higher absolute values of binding energies.

Effect of DYGXN on Lipid Metabolism in Mice

The serum lipid profile results showed that, compared to the control group, the model group had significantly higher levels of LDL-C, TC, non-HDL-C and TG ($P < 0.001$, $P < 0.001$, $P < 0.001$, $P < 0.001$), while HDL-C levels were significantly lower ($P < 0.01$). Compared to the model group, both DYGXN and rosuvastatin significantly reduced serum LDL-C levels ($P < 0.05$) and increased HDL-C levels ($P < 0.01$). Rosuvastatin significantly reduced non-HDL-C and TC levels ($P < 0.05$, $P < 0.05$). DYGXN exhibited a trend towards lowering TC, non-HDL-C and TG levels, but the difference was not statistically significant (Figure 11).

Effect of DYGXN on Serum Inflammatory Cytokines

The results of serum inflammatory cytokine measurements indicated that, compared with the control group, the model group showed a significant increase in serum levels of NF-κB, IL-6, ICAM-1, and IL-1β ($P < 0.05$, $P < 0.001$, $P < 0.05$, $P < 0.001$). TNF-α and ICAM-1 showed an upward trend, but the differences were not statistically significant. Compared with the model group, the DYGXN and rosuvastatin groups exhibited significant reductions in NF-κB, IL-6, and IL-1β levels, with statistically significant differences ($P < 0.01$, $P < 0.001$, $P < 0.001$). However, there were no statistically significant differences in the levels of TNF-α, ICAM-1, and VCAM-1 (Figure 12).

Effect of DYGXN on the Expression of p-Src/Src, p-STAT3/STAT3

Western blot results showed that compared to the control group, high-fat diet feeding of $ApoE^{-/-}$ mice promoted the expression of p-Src and p-STAT3 proteins in the aorta ($P < 0.001$). After intervention with DYGXN, the expression of p-Src and p-STAT3 proteins was significantly reduced ($P < 0.05$, $P < 0.001$) (Figure 13).

https://doi.org/10.2147/JIR.S511604

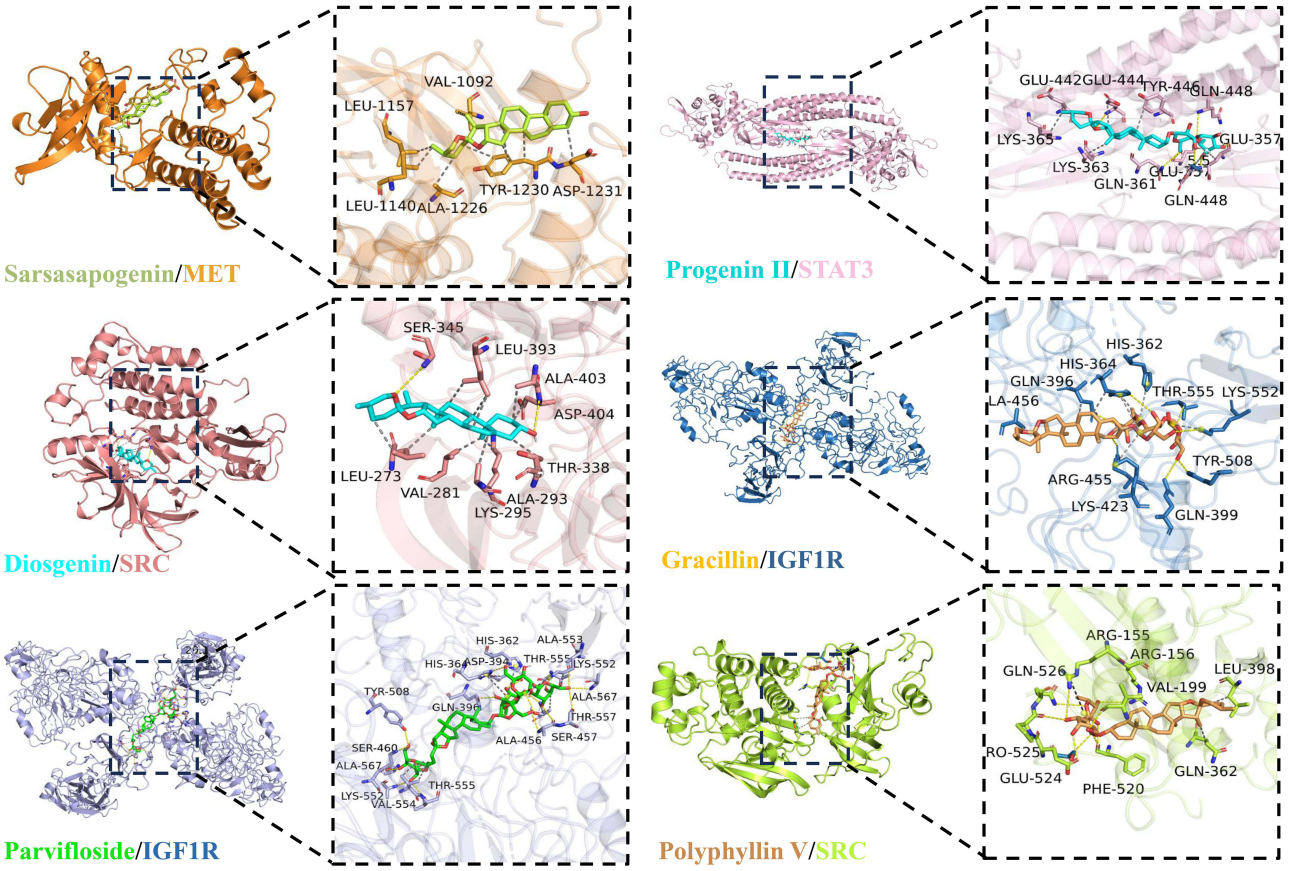

Figure 8 Representative docking models. From top to bottom: the molecular docking results of sarsasapogenin with MET, progenin II with STAT3, diosgenin with SRC, gracillin with IGF1R, parvifloside with IGF1R, and polyphyllin V with SRC. Yellow represents hydrogen bonds, and gray indicates van der Waals forces.

Discussion

AS is a chronic inflammatory disease of the vascular wall driven by lipid accumulation, primarily occurring in the subendothelial space of medium- to large-sized arteries, particularly at sites of disturbed blood flow or branching points.[31] Major risk factors for AS include high-fat diets, hypertension, hyperglycemia, and smoking. This disease progresses through several stages. In the early stage, lipid deposits accumulate beneath the intima, leading to the formation of fatty streaks. As lipid deposition increases, these streaks soften and evolve into yellow plaques. In the later stages, the plaques become raised and their color changes to white or gray, with the accumulation of cholesterol crystals within the plaques. In the final stages, calcification occurs, leading to plaque rupture, the formation of atherosclerotic ulcers, and potentially thrombus formation, which can occlude blood vessels and trigger a series of cardiovascular events.[32,33] The genus Dioscorea have a long history of use in China. DYGXN is a water-soluble steroidal saponin extract from *Dioscorea zingiberensis*. Previous studies have shown that DYGXN effectively treats coronary heart disease and improves hyperlipidemia, demonstrating positive effects on AS. However, there is currently limited research on the specific mechanisms through which DYGXN exerts its anti- AS effects.

Active Component Analysis of DYGXN

Compared to traditional network pharmacology, which analyzes drug components and predicts targets through databases, network pharmacology based on the chemical composition analysis and identification of drug components is more scientific and reliable. In this study, UPLC-Q-Orbitrap HR-MS technology was used for qualitative analysis of the chemical components of DYGXN. A total of 20 compounds were identified or predicted, including 3 saponins: diosgenin, sarsasapogenin, and tigogenin. Diosgenin may be the primary active component responsible for the anti-AS effects of DYDXN. Several studies have confirmed that diosgenin is the main metabolic component of steroidal saponins

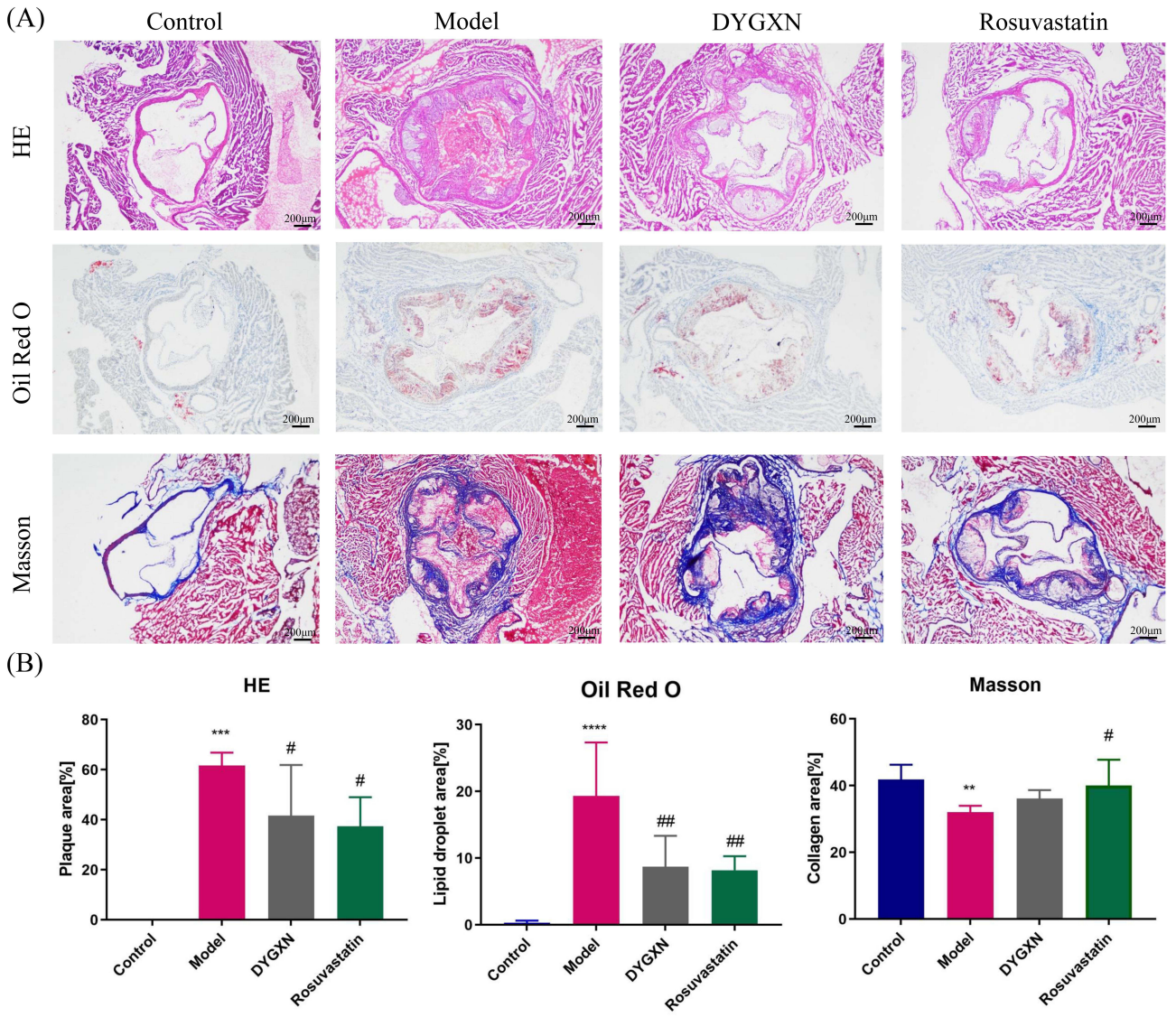

Figure 9 Anti-AS effects of DYGXN. (**A**) Representative images of HE staining, Oil Red O staining, and Masson staining of aortic root sections. (**B**) Quantification of aortic root plaque area, lipid droplet content, and collagen fiber area. Compared to the control group, $^{**}P < 0.01$; $^{***}P < 0.001$; $^{****}P < 0.0001$; compared to the model group, $^{\#}P < 0.05$, $^{\#\#}P < 0.01$. n = 6, scale bar: 200 μm.

from *Dioscorea* species. For example, Feng JF et al showed that *Dioscorea nipponica* can be metabolized into diosgenin under the influence of gut microbiota.[34] After administering total saponins from *Dioscorea zingiberensis* to rats via gavage, Qin Y used ESI-QTOF-MS technology to analyze rat plasma and found that only diosgenin was detected.[35] A comparative study on the metabolism of total saponins from three species of the genus Dioscorea (*Dioscorea panthaica* Prain et Burkill, *Dioscorea zingiberensis* C. H. Wrigh, and *Dioscorea nipponica* Makino) and four specific saponins (diosgenin, protodioscin, pseudoprotodioscin and dioscin) in rat plasma was conducted. The study detected a total of 10 saponin components in rat plasma and urine, and 18 saponin components in the feces. Additionally, they observed that the conversion rate of diosgenin increased over time, indicating that the deglycosylation to diosgenin is the main metabolic pathway of steroidal saponins.[36] Among the compounds of DYGXN, various steroidal saponins with diosgenin as the core structure were identified, such as dioscin, protodioscin, pseudoprotodioscin, Methyl protodioscin. Based on these findings, we speculate that the multiple steroidal saponins in DYGXN may be converted into diosgenin through deglycosylation and other metabolic processes in the intestine or plasma, and diosgenin is likely to be the active component responsible for the anti- AS effects of DYGXN.

https://doi.org/10.2147/JIR.S511604

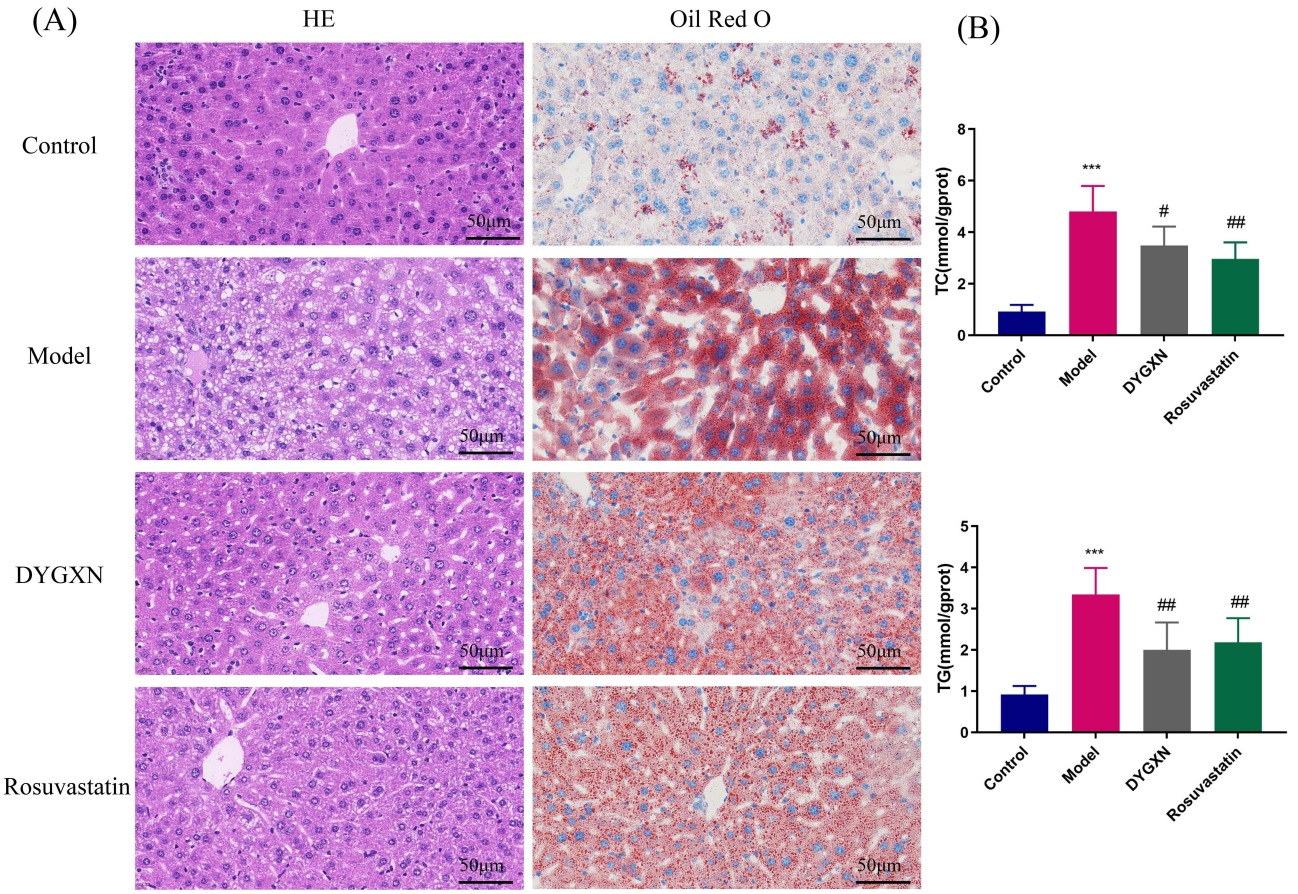

Figure 10 Effects of DYGXN on liver tissue morphology and lipid accumulation. (**A**) Representative images of HE staining and Oil Red O staining of liver sections. (**B**) Quantification of liver TC and TG levels. Compared to the control group, ***P < 0.001. Compared to the model group, #P < 0.05, ##P < 0.01. n = 6. scale bar: 50 μm.

Several studies have demonstrated the positive anti-AS effects of diosgenin. For example, Lv YC et al found that diosgenin promotes ATP-binding cassette transporter A1 (ABCA1) protein expression through multiple pathways, enhancing cholesterol efflux and alleviating AS.[37] Jung DH et al reported that diosgenin inhibits the activation of NF-κB, activating protein-1 (AP-1), casein kinase 2 (CK2), and c-Jun N-terminal kinase (JNK), thereby reducing the production of pro-inflammatory cytokines.[38] Diosgenin also promotes the polarization of ox-LDL-treated monocytes into M2-type macrophages, exerting anti-inflammatory effects.[39] In addition to diosgenin, several other components in DYGXN have been shown to possess anti-AS effects. For example, dioscin can regulate gastrointestinal function, promote the transformation of beneficial gut microbiota, and improve hyperlipidemia.[40] It also enhances antioxidant enzyme expression and reduces oxidative stress,[41] and inhibits the NF-κB signaling pathway, reducing TNF-α expression and suppressing atherosclerotic inflammation.[42] Sarsasapogenin has been shown to possess significant anti-inflammatory effects.[43] It inhibits the expression of matrix metalloproteinase-2 (MMP2) and MMP9 in vascular smooth muscle cells (VSMCs), and simultaneously suppresses the expression of stromal interaction molecule 1 (STIM1) and Orai, reducing ox-LDL-induced proliferation, migration, and invasion of VSMCs, thus exerting anti-AS effects.[44] Methyl protodioscin and Pseudoprotodioscin can lower LDL-C and triglyceride levels, promote HDL-C levels, and increase ABCA1 and Apolipoprotein A-1(ApoA-1) expression by inhibiting sterol regulatory element-binding protein (SREBP), microRNA 33a/b, and protein convertase subtilisin/kexin type 9 (PCSK9), thereby promoting cholesterol efflux and improving AS.[45,46] Pseudoprotodioscin reduces inflammation in perivascular adipose tissue, promotes estrogen receptor expression, exerts anti-inflammatory and estrogenic effects, and decreases plaque area in ovariectomized ApoE$^{-/-}$ mice.[47] Trillin reduces total cholesterol and triglyceride levels in the blood, alleviates lipid peroxidation, improves hyperlipidemia in rats, and exhibits biological activity similar to that of lovastatin.[48]

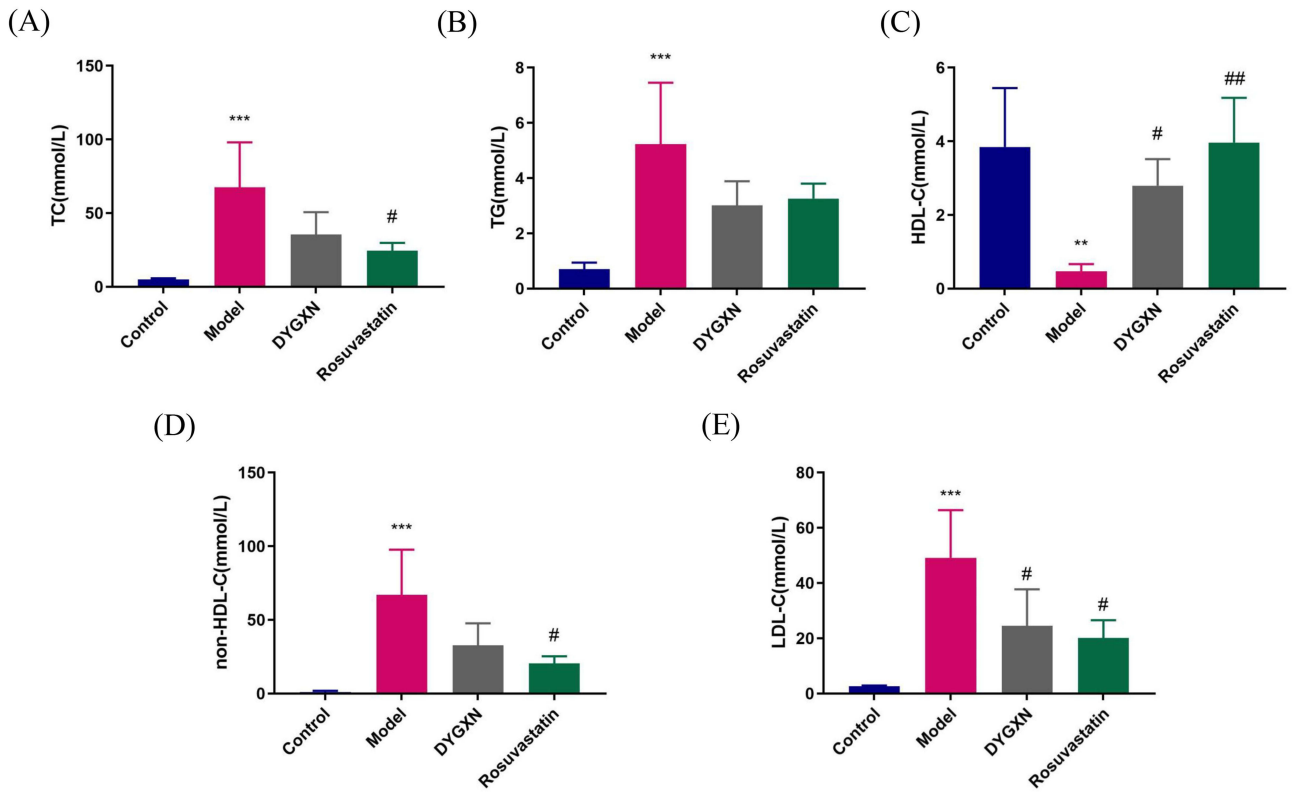

Figure 11 Serum lipid levels of mice after 12 weeks of treatment. DYGXN reduces LDL-C and promotes HDL-C, with little effect on TC, non-HDL-C and TG. (**A**) The serum TC level of mice. (**B**) The serum TG level of mice. (**C**) The serum HDL-C level of mice. (**D**) The serum non-HDL-C level of mice. (**E**) The serum LDL-C level of mice. Compared to the control group, $^{**}P < 0.01$, $^{***}P < 0.001$; compared to the model group, $^{\#}P < 0.05$, $^{\#\#}P < 0.01$, n = 4.

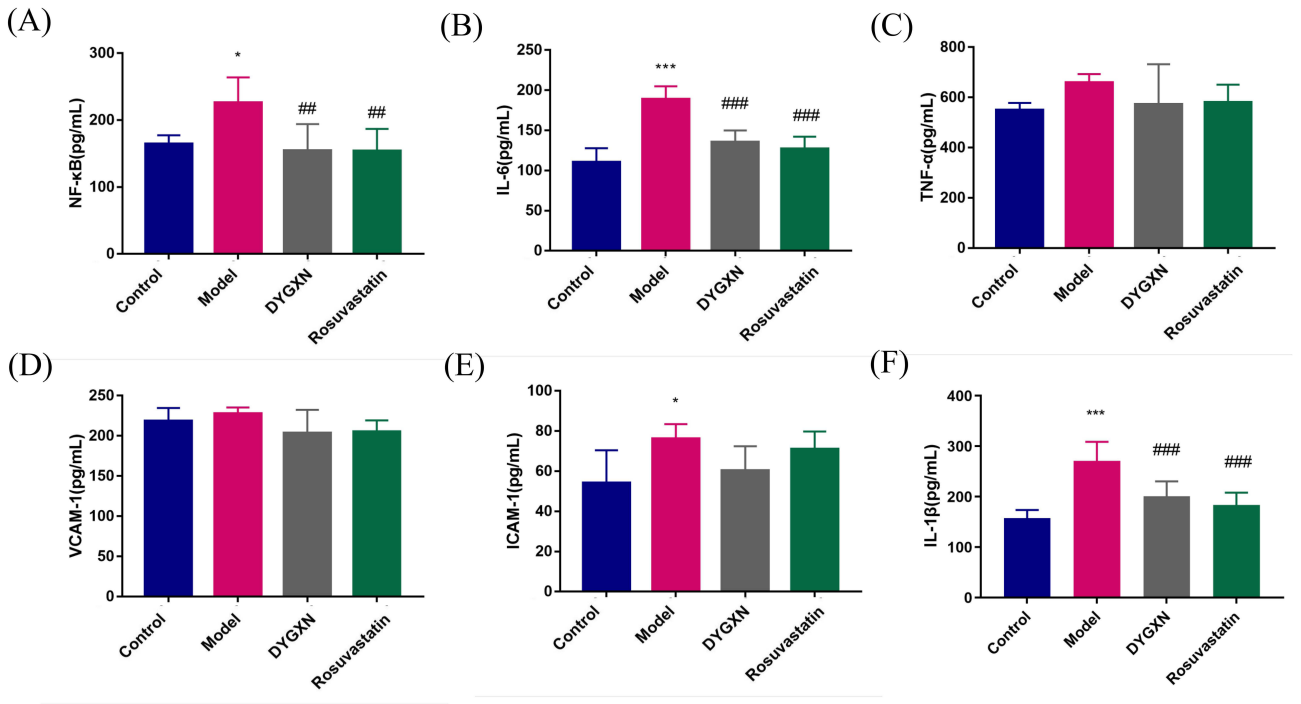

Figure 12 Serum inflammatory cytokine levels after 12 weeks of treatment in different groups of mice. DYGXN decreased the levels of NF-κB, IL-6 and IL-1β, with little effect on TNF-α, ICAM-1 and VCAM-1. (**A**) The serum NF-κB level of mice. (**B**) The serum IL-6 level of mice. (**C**) The serum TNF-α level of mice. (**D**) The serum VCAM-1 level of mice. (**E**) The serum ICAM-1 level of mice. (**F**) The serum IL-1β level of mice. Compared to the control group, $^{*}P < 0.05$; $^{***}P < 0.001$; compared to the model group, $^{\#\#}P < 0.01$, $^{\#\#\#}P < 0.001$, n = 6.

https://doi.org/10.2147/JIR.S511604

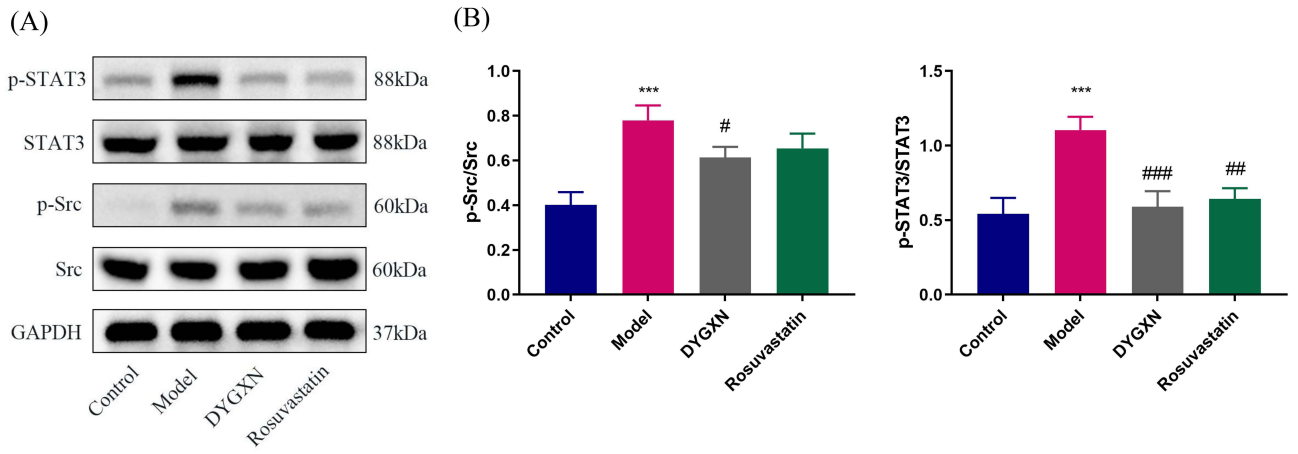

Figure 13 Effect of DYGXN on the expression of p-Src, Src, p-STAT3, and STAT3 proteins in the aorta of mice. (**A**) Representative Western blot images of p-Src, Src, p-STAT3, and STAT3. (**B**) Relative protein expression levels. Compared to the control group, ***P < 0.001; compared to the model group, #P < 0.05, ##P < 0.01, ###P < 0.001, n=3.

Key Target Analysis

After identifying the components of DYGXN, our study explores the anti-AS mechanism of DYGXN through network pharmacology, molecular docking, and animal experiments. First, common targets of DYGXN components and AS were predicted using multiple databases, and a PPI network was constructed to screen and identify 10 core target genes. Among them, signal transducer and activator of transcription 3 (STAT3) and proto-oncogene tyrosine-protein kinase SRC (SRC) showed the highest degree values and were located in the lipid and atherosclerosis pathway identified by KEGG enrichment. Therefore, STAT3 and SRC are likely to be the primary targets through which DYGXN exerts its anti- AS effects. Previous studies have shown that STAT3 is an important protein in cell signaling and transcription, and is highly expressed in human atherosclerotic macrophages. It can promote AS by inducing macrophage pyroptosis, enhancing endothelial cell dysfunction, macrophage polarization, inflammation, and immune response.[49,50] Additionally, Shen W et al found that the inclusion of diosgenin in the diet can target and inhibit the transcriptional activity of STAT3, leading to a reduction in Niemann-Pick C1-like 1(NPC1L1) expression and inhibiting intestinal cholesterol absorption.[51] Targeting STAT3 may represent a potential therapeutic strategy for the treatment of AS.[52] Src, a non-receptor tyrosine kinase associated with cell migration, plays various roles in macrophage-mediated inflammatory responses and innate immunity.[53] Studies have shown that Src is involved in regulating inflammation pathways mediated by all members of the toll-like receptors (TLR) family, and it can also promote lipid accumulation in macrophages[54] and induce endothelial barrier dysfunction.[55] Inhibition of the Src-Yap signaling pathway has been shown to reduce endothelial cell inflammation and improve AS.[56] Src has been identified as an atypical kinase of STAT3,[57] and recently, the Src/STAT3 pathway has been found to promote tumor angiogenesis,[58] as well as cancer cell proliferation and invasion.[59] Given the critical roles of Src and STAT3 in inflammation, we hypothesize that the Src/STAT3 pathway may contribute to the development of AS, and that DYGXN may exert its anti-AS effects by modulating this pathway.

Biological Enrichment Analysis

GO functional analysis indicates that DYGXN exerts its anti-AS effects by modulating biological processes such as phosphorylation, positive regulation of kinase activity, negative regulation of the apoptotic process, angiogenesis, cell migration, and inflammatory response. KEGG enrichment analysis revealed that the target proteins are enriched in several cancer-related signaling pathways, such as Pathways in Cancer, Kaposi Sarcoma-associated Herpesvirus Infection, and MicroRNAs in Cancer. This suggests that multiple targets (eg, SRC, STAT3, etc). are involved in both cancer and AS-related signaling pathways, exhibiting some mechanistic similarities, such as the inhibition of angiogenesis, suppression of cell proliferation and migration, and the reduction of inflammation. After excluding these cancer-related pathways, we found that the anti-AS mechanisms of DYGXN are primarily associated with the Rap1 signaling pathway, MAPK signaling pathway, lipid and atherosclerosis, and the JAK-STAT signaling pathway and so on. Among

these, the MAPK signaling pathway can induce AS through various mechanisms, including the regulation of macrophage polarization,[60] promotion of inflammation and apoptosis,[61] and the stimulation of smooth muscle cell proliferation and migration.[62] The Rap1 signaling pathway is involved in the regulation of cell adhesion and cell-cell junctions. Studies have shown that ras-associated protein 1 (Rap1) accumulates in plaques, where it promotes the proliferation and migration of VSMCs, exacerbates endothelial inflammation, and accelerates AS.[63,64] The JAK-STAT signaling pathway inhibits cholesterol efflux by downregulating ABCA1,[65] and also exacerbates AS by promoting inflammation.[66] Currently, controlling cholesterol and LDL-C levels remains the primary strategy for preventing and treating AS, which aligns with DYGXN's ability to regulate lipid and atherosclerosis pathway.

Experimental Results Analysis

Animal experiments showed that DYGXN significantly reduced serum LDL-C levels and increased HDL-C levels, suggesting that DYGXN may prevent the progression of AS in mice by improving hyperlipidemia. Histopathological staining confirmed that DYGXN intervention significantly reduced the area of AS plaques, decreased lipid deposition in plaques, and delayed AS progression. Liver histopathological staining indicated that DYGXN reduced hepatic pathological damage and hepatic lipid accumulation, lowering liver cholesterol and triglyceride levels. Additionally, DYGXN significantly decreased serum NF-κB, IL-6, and IL-1β levels, and reduced inflammatory cell infiltration in aortic roots, suggesting that DYGXN may prevent AS progression by inhibiting NF-κB signaling pathway and suppressing the expression of inflammatory cytokines. Furthermore, Western blot analysis showed that DYGXN inhibited the phosphorylation of Src and STAT3 proteins in the aorta, indicating that DYGXN may exert its anti-AS effect by inhibiting the Src/STAT3 signaling pathway, improving inflammation and lipid metabolism. However, further studies are needed to confirm this conclusion.

However, this study also has some limitations. For example, due to insufficient reference standards, highly similar isomer fragmentation pathways, or unclear ion abundance, it was challenging to distinguish some isomers using mass spectrometry. Moreover, this study did not conduct quantitative detection of DYGXN components nor analyze the components that entered the bloodstream. Additionally, animal experiments did not include low, medium, and high-dose groups to further explore the optimal dosing regimen of DYGXN in mice and comprehensively assess the dose - response relationship, and the mechanisms were not deeply validated, which are areas for further improvement in future research.

Conclusion

In conclusion, this study is the first to reveal the compounds of DYGXN and provides a preliminary exploration of its pharmacological basis, laying an important foundation for the screening of quality markers. By combining network pharmacology, we identified the active components and core targets of DYGXN in the treatment of AS, further elucidating the correlation between DYGXN and its clinical efficacy in AS. Moreover, molecular docking techniques were used to validate the predicted results, offering a preliminary exploration of the material basis and molecular mechanisms underlying DYGXN's anti-AS effects. Animal experiments were conducted to verify its anti-AS effects and potential mechanisms, which provided a theoretical foundation for further investigation into the mechanism of the anti-AS effects of DYGXN. In conclusion, the results of this study demonstrate that DYGXN contains multiple active components that exert anti-AS effects by regulating various targets and pathways.

Abbreviations

AS, atherosclerosis; DYGXN, Dunyeguanxinning; SOD, Superoxide dismutase; NF-κB, Nuclear factor kappa B; IL-1β, Interleukin 1 Beta; IL-6, Interleukin 6; TNF-α, Tumor Necrosis Factor Alpha; ICAM-1, Intercellular adhesion molecule-1; VCAM-1, Vascular cellular adhesion molecule-1; ApoA-1, Apolipoprotein A-1; STIM1, Stromal interaction molecule 1; MMP, Matrix metalloproteinase; NPC1L1, Niemann-Pick C1-Like 1; STAT3, signal transducer and activator of transcription 3; Src, proto-oncogene tyrosine-protein kinase SRC; TLR, toll-like receptors; Rap1, Ras-associated protein 1; ABCA1, ATP-binding cassette transporter A1; SREBP, sterol regulatory element-binding protein; PCSK9, protein convertase subtilisin/kexin type 9; CK2, casein kinase 2; AP-1, activating protein-1; JNK, c-Jun N-terminal kinase.

Ethics Statement

All animal experiments were conducted in accordance with the Laboratory Animal-Guideline for Ethical Review of Animal Welfare (GB/T 35892–2018) and were approved by the Ethics Committee of Shanghai University of Traditional Chinese Medicine (ethics approval number: PZSHUTCM220627030). According to China's "Ethical Review Measures for Life Sciences and Medical Research Involving Humans," human databases involved in research are exempt from the scope of ethical approval.

Funding

This work was supported by Shanghai Medical Innovation Research Project (Major Project) (No. 23Y31920200), Shanghai Key Laboratory of Traditional Chinese Clinical Medicine(20DZ2272200) and National Natural Science Foundation of China (No. 82074222 and No. 82374252).

Disclosure

All the authors declare that there are no conflicts of interest in this work.

References

1. Tsao CW, Aday AW, Almarzooq ZI. et al. Heart Disease and Stroke Statistics-2022 Update: a Report From the American Heart Association. *Circulation*. 2022;145(8):e153–e639. doi:10.1161/CIR.0000000000001052
2. Roth GA, Mensah GA, Johnson CO, et al. Global Burden of Cardiovascular Diseases and Risk Factors, 1990–2019: update From the GBD 2019 Study. *J Am Coll Cardiol*. 2020;76(25):2982–3021. doi:10.1016/j.jacc.2020.11.010
3. Mathers CD, Loncar D. Projections of global mortality and burden of disease from 2002 to 2030. *PLoS Med*. 2006;3(11):e442. doi:10.1371/journal.pmed.0030442
4. Libby P, Buring JE, Badimon L, et al. Atherosclerosis. *Nat Rev Dis Primers*. 2019;5(1):56. doi:10.1038/s41572-019-0106-z
5. Tomaszewski M, Stepien KM, Tomaszewska J, Czuczwar SJ. Statin-induced myopathies. *Pharmacol Rep*. 2011;63(4):859–866. doi:10.1016/S1734-1140(11)70601-6
6. Ward NC, Pang J, Ryan JDM, Watts GF. Nutraceuticals in the management of patients with statin-associated muscle symptoms, with a note on real-world experience. *Clin Cardiol*. 2018;41(1):159–165. doi:10.1002/clc.22862
7. Cai G, Zhou W, Lu Y, Chen P, Lu Z, Fu Y. Aspirin resistance and other aspirin-related concerns. *Neurol Sci*. 2016;37(2):181–189. doi:10.1007/s10072-015-2412-x
8. Sostres C, Lanas A. Gastrointestinal effects of aspirin. *Nat Rev Gastroenterol Hepatol*. 2011;8(7):385–394. doi:10.1038/nrgastro.2011.97
9. Pan CH, Tsai CH, Liu FC, et al. Influence of different particle processing on hypocholesterolemic and antiatherogenic activities of yam (Dioscorea pseudojaponica) in cholesterol-fed rabbit model. *J Sci Food Agric*. 2013;93(6):1278–1283. doi:10.1002/jsfa.5882
10. Koo HJ, Park HJ, Byeon HE, et al. Chinese yam extracts containing beta-sitosterol and ethyl linoleate protect against atherosclerosis in apolipoprotein E-deficient mice and inhibit muscular expression of VCAM-1 in vitro. *J Food Sci*. 2014;79(4):H719–729. doi:10.1111/1750-3841.12401
11. Zhang X, Jin M, Tadesse N, et al. Dioscorea zingiberensis C. H. Wright: an overview on its traditional use, phytochemistry, pharmacology, clinical applications, quality control, and toxicity. *J Ethnopharmacol*. 2018;220:283–293. doi:10.1016/j.jep.2018.03.017
12. Zhang R, Huang B, Du D, et al. Anti-thrombosis effect of diosgenyl saponins in vitro and in vivo. *Steroids*. 2013;78(11):1064–1070. doi:10.1016/j.steroids.2013.07.003
13. Dan L, Hua WX, Yang H, Wen H, Zhihua I. Preventive effects of water extracts from Dioscorea zingiberensis on athersclerosis formation in rabbits. *West China Journal of Pharmaceutical Sciences*. 2011;26(02):144–146.
14. Du Fuchang et al Dept of Cardiovascular Diseases, The First Affiliated Hospital NMCTCGoDYGP. The Therapeutic Effects of Protozingiberenin A & B (Deng ye Guanxinning Pian) in 90 Cases of Coronary Heart Disease. *Jiangsu Med J*. 1985;11:16–19.
15. Yiping L, Xiaofen R, Xiaolong W. Efficacy and Safety of Dunye Guanxinning in the Treatment of Coronary Heart Disease and Angina Pectoris:a Meta-analysis. *Chin J Integrat Med Cardio-Cerebrovas Dis*. 2017;15(19):2376–2380.
16. Nogales C, Mamdouh ZM, List M, Kiel C, Casas AI, Schmidt H. Network pharmacology: curing causal mechanisms instead of treating symptoms. *Trends Pharmacol Sci*. 2022;43(2):136–150. doi:10.1016/j.tips.2021.11.004
17. Hopkins AL. Network pharmacology: the next paradigm in drug discovery. *Nat Chem Biol*. 2008;4(11):682–690. doi:10.1038/nchembio.118
18. Kibble M, Saarinen N, Tang J, Wennerberg K, Makela S, Aittokallio T. Network pharmacology applications to map the unexplored target space and therapeutic potential of natural products. *Nat Prod Rep*. 2015;32(8):1249–1266. doi:10.1039/c5np00005j
19. Shu X, Xu R, Xiong P, et al. Exploring the Effects and Potential Mechanisms of Hesperidin for the Treatment of CPT-11-Induced Diarrhea: network Pharmacology, Molecular Docking, and Experimental Validation. *Int J mol Sci*. 2024;25(17):9309.
20. Dai L, Cai S, Chu D, et al. Identification of Chemical Constituents in Blumea balsamifera Using UPLC-Q-Orbitrap HRMS and Evaluation of Their Antioxidant Activities. *Molecules*. 2023;28(11):4504.
21. Daina A, Michielin O, Zoete V. SwissTargetPrediction: updated data and new features for efficient prediction of protein targets of small molecules. *Nucleic Acids Res*. 2019;47(W1):W357–W364. doi:10.1093/nar/gkz382
22. Safran M, Dalah I, Alexander J, et al. GeneCards Version 3: the human gene integrator. *Database*. 2010;2010:baq020. doi:10.1093/database/baq020
23. Amberger JS, Bocchini CA, Scott AF, Hamosh A. OMIM.org: leveraging knowledge across phenotype-gene relationships. *Nucleic Acids Res*. 2019;47(D1):D1038–D1043. doi:10.1093/nar/gky1151

24. Zhou Y, Zhang Y, Zhao D, et al. TTD: therapeutic Target Database describing target druggability information. *Nucleic Acids Res*. 2024;52(D1): D1465–D1477. doi:10.1093/nar/gkad751
25. Wishart DS, Feunang YD, Guo AC, et al. DrugBank 5.0: a major update to the DrugBank database for 2018. *Nucleic Acids Res*. 2018;46(D1): D1074–D1082. doi:10.1093/nar/gkx1037
26. Pinero J, Sauch J, Sanz F, Furlong LI. The DisGeNET cytoscape app: exploring and visualizing disease genomics data. *Comput Struct Biotechnol J*. 2021;19:2960–2967. doi:10.1016/j.csbj.2021.05.015
27. Szklarczyk D, Gable AL, Nastou KC, et al. The STRING database in 2021: customizable protein-protein networks, and functional characterization of user-uploaded gene/measurement sets. *Nucleic Acids Res*. 2021;49(D1):D605–D612. doi:10.1093/nar/gkaa1074
28. Huang DW, Sherman BT, Tan Q, et al. DAVID Bioinformatics Resources: expanded annotation database and novel algorithms to better extract biology from large gene lists. *Nucleic Acids Res*. 2007;35(Web Server issue):W169–175. doi:10.1093/nar/gkm415
29. Bardou P, Mariette J, Escudie F, Djemiel C, Klopp C. jvenn: an interactive Venn diagram viewer. *BMC Bioinf*. 2014;15(1):293. doi:10.1186/1471-2105-15-293
30. Gaillard T. Evaluation of AutoDock and AutoDock Vina on the CASF-2013 Benchmark. *J Chem Inf Model*. 2018;58(8):1697–1706. doi:10.1021/acs.jcim.8b00312
31. Weber C, Noels H. Atherosclerosis: current pathogenesis and therapeutic options. *Nat Med*. 2011;17(11):1410–1422. doi:10.1038/nm.2538
32. Badimon L, Vilahur G. Thrombosis formation on atherosclerotic lesions and plaque rupture. *J Intern Med*. 2014;276(6):618–632. doi:10.1111/joim.12296
33. Dron JS, Lazarte J, Hegele RA. Recent Highlights of ATVB. *Arterioscler Thromb Vasc Biol*. 2018;38(11):e185–e197. doi:10.1161/ATVBAHA.118.311581
34. Feng JF, Tang YN, Ji H, Xiao ZG, Zhu L, Yi T. Biotransformation of Dioscorea nipponica by Rat Intestinal Microflora and Cardioprotective Effects of Diosgenin. *Oxid Med Cell Longev*. 2017;2017(1):4176518. doi:10.1155/2017/4176518
35. Qin Y, Wu X, Huang W, et al. Acute toxicity and sub-chronic toxicity of steroidal saponins from Dioscorea zingiberensis C.H.Wright in rodents. *J Ethnopharmacol*. 2009;126(3):543–550. doi:10.1016/j.jep.2009.08.047
36. Tang YN, Pang YX, He XC, et al. UPLC-QTOF-MS identification of metabolites in rat biosamples after oral administration of Dioscorea saponins: a comparative study. *J Ethnopharmacol*. 2015;165:127–140. doi:10.1016/j.jep.2015.02.017
37. Lv YC, Yang J, Yao F, et al. Diosgenin inhibits atherosclerosis via suppressing the MiR-19b-induced downregulation of ATP-binding cassette transporter A1. *Atherosclerosis*. 2015;240(1):80–89. doi:10.1016/j.atherosclerosis.2015.02.044
38. Jung DH, Park HJ, Byun HE, et al. Diosgenin inhibits macrophage-derived inflammatory mediators through downregulation of CK2, JNK, NF-kappaB and AP-1 activation. *Int Immunopharmacol*. 2010;10(9):1047–1054. doi:10.1016/j.intimp.2010.06.004
39. Binesh A, Devaraj SN, Devaraj H. Expression of chemokines in macrophage polarization and downregulation of NFkappaB in aorta allow macrophage polarization by diosgenin in atherosclerosis. *J Biochem mol Toxicol*. 2020;34(2):e22422. doi:10.1002/jbt.22422
40. Jeon JR, Lee JS, Lee CH, Kim JY, Kim SD, Nam DH. Effect of ethanol extract of dried Chinese yam (Dioscorea batatas) flour containing dioscin on gastrointestinal function in rat model. *Arch Pharm Res*. 2006;29(5):348–353. doi:10.1007/BF02968583
41. Qiao Y, Xu L, Tao X, et al. Protective effects of dioscin against fructose-induced renal damage via adjusting Sirt3-mediated oxidative stress, fibrosis, lipid metabolism and inflammation. *Toxicol Lett*. 2018;284:37–45. doi:10.1016/j.toxlet.2017.11.031
42. Wu S, Xu H, Peng J, et al. Potent anti-inflammatory effect of dioscin mediated by suppression of TNF-alpha-induced VCAM-1, ICAM-1and EL expression via the NF-kappaB pathway. *Biochimie*. 2015;110:62–72. doi:10.1016/j.biochi.2014.12.022
43. Yu YY, Cui SC, Zheng TN, et al. Sarsasapogenin improves adipose tissue inflammation and ameliorates insulin resistance in high-fat diet-fed C57BL/6J mice. *Acta Pharmacol Sin*. 2021;42(2):272–281. doi:10.1038/s41401-020-0427-1
44. Zhai H, Liu H, Shang B, Zou X. Sarsasapogenin blocks ox-LDL-stimulated vascular smooth muscle cell proliferation, migration, and invasion through suppressing STIM1 expression. *Cardiovasc Diagn Ther*. 2023;13(3):441–452. doi:10.21037/cdt-23-111
45. Ma W, Ding H, Gong X, et al. Methyl protodioscin increases ABCA1 expression and cholesterol efflux while inhibiting gene expressions for synthesis of cholesterol and triglycerides by suppressing SREBP transcription and microRNA 33a/b levels. *Atherosclerosis*. 2015;239(2):566–570. doi:10.1016/j.atherosclerosis.2015.02.034
46. Gai Y, Li Y, Xu Z, Chen J. Pseudoprotodioscin inhibits SREBPs and microRNA 33a/b levels and reduces the gene expression regarding the synthesis of cholesterol and triglycerides. *Fitoterapia*. 2019;139:104393. doi:10.1016/j.fitote.2019.104393
47. Sun B, Yang D, Yin YZ, Xiao J. Estrogenic and anti-inflammatory effects of pseudoprotodioscin in atherosclerosis-prone mice: insights into endothelial cells and perivascular adipose tissues. *Eur J Pharmacol*. 2020;869:172887. doi:10.1016/j.ejphar.2019.172887
48. Wang T, Choi RC, Li J, et al. Trillin, a steroidal saponin isolated from the rhizomes of Dioscorea nipponica, exerts protective effects against hyperlipidemia and oxidative stress. *J Ethnopharmacol*. 2012;139(1):214–220. doi:10.1016/j.jep.2011.11.001
49. Yang L, Song Z, Pan Y, et al. PM (2.5) promoted lipid accumulation in macrophage via inhibiting JAK2/STAT3 signaling pathways and aggravating the inflammatory reaction. *Ecotoxicol Environ Saf*. 2021;226:112872. doi:10.1016/j.ecoenv.2021.112872
50. Wei Y, Lan B, Zheng T, et al. GSDME-mediated pyroptosis promotes the progression and associated inflammation of atherosclerosis. *Nat Commun*. 2023;14(1):929. doi:10.1038/s41467-023-36614-w
51. Shen W, Shao W, Wang Q, et al. Dietary diosgenin transcriptionally down-regulated intestinal NPC1L1 expression to prevent cholesterol gallstone formation in mice. *J Biomed Sci*. 2023;30(1):44. doi:10.1186/s12929-023-00933-3
52. Chen Q, Lv J, Yang W, et al. Targeted inhibition of STAT3 as a potential treatment strategy for atherosclerosis. *Theranostics*. 2019;9 (22):6424–6442. doi:10.7150/thno.35528
53. Byeon SE, Yi YS, Oh J, Yoo BC, Hong S, Cho JY. The role of Src kinase in macrophage-mediated inflammatory responses. *Mediators Inflamm*. 2012;2012:512926. doi:10.1155/2012/512926
54. Yang K, Wang X, Liu Z, et al. Oxidized low-density lipoprotein promotes macrophage lipid accumulation via the toll-like receptor 4-Src pathway. *Circ J*. 2015;79(11):2509–2516. doi:10.1253/circj.CJ-15-0345
55. Sun C, Wu MH, Lee ES, Yuan SY. A disintegrin and metalloproteinase 15 contributes to atherosclerosis by mediating endothelial barrier dysfunction via Src family kinase activity. *Arterioscler Thromb Vasc Biol*. 2012;32(10):2444–2451. doi:10.1161/ATVBAHA.112.252205
56. Ding H, Jiang M, Lau CW, et al. Curaxin CBL0137 inhibits endothelial inflammation and atherogenesis via suppression of the Src-YAP signalling axis. *Br J Pharmacol*. 2023;180(8):1168–1185. doi:10.1111/bph.16007

57. Schreiner SJ, Schiavone AP, Smithgall TE. Activation of STAT3 by the Src family kinase Hck requires a functional SH3 domain. *J Biol Chem*. 2002;277(47):45680–45687. doi:10.1074/jbc.M204255200
58. Liu YX, Xu BW, Niu XD, et al. Inhibition of Src/STAT3 signaling-mediated angiogenesis is involved in the anti-melanoma effects of dioscin. *Pharmacol Res*. 2022;175:105983. doi:10.1016/j.phrs.2021.105983
59. Deng B, Jiang XL, Tan ZB, et al. Dauricine inhibits proliferation and promotes death of melanoma cells via inhibition of Src/STAT3 signaling. *Phytother Res*. 2021;35(7):3836–3847. doi:10.1002/ptr.7089
60. Jin Z, Li J, Pi J, et al. Geniposide alleviates atherosclerosis by regulating macrophage polarization via the FOS/MAPK signaling pathway. *Biomed Pharmacother*. 2020;125:110015. doi:10.1016/j.biopha.2020.110015
61. Gong L, Lei Y, Liu Y, et al. Vaccarin prevents ox-LDL-induced HUVEC EndMT, inflammation and apoptosis by suppressing ROS/p38 MAPK signaling. *Am J Transl Res*. 2019;11(4):2140–2154.
62. Miyabe M, Nakamura N, Saiki T, et al. Porphyromonas gingivalis Lipopolysaccharides Promote Proliferation and Migration of Human Vascular Smooth Muscle Cells through the MAPK/TLR4 Pathway. *Int J mol Sci*. 2022;24(1):125. doi:10.3390/ijms24010125
63. Perdomo L, Vidal-Gomez X, Soleti R, et al. Large Extracellular Vesicle-Associated Rap1 Accumulates in Atherosclerotic Plaques, Correlates With Vascular Risks and Is Involved in Atherosclerosis. *Circ Res*. 2020;127(6):747–760. doi:10.1161/CIRCRESAHA.120.317086
64. Singh B, Kosuru R, Lakshmikanthan S, et al. Endothelial Rap1 (Ras-Association Proximate 1) Restricts Inflammatory Signaling to Protect From the Progression of Atherosclerosis. *Arterioscler Thromb Vasc Biol*. 2021;41(2):638–650. doi:10.1161/ATVBAHA.120.315401
65. Mo ZC, Xiao J, Liu XH, et al. AOPPs inhibits cholesterol efflux by down-regulating ABCA1 expression in a JAK/STAT signaling pathway-dependent manner. *J Atheroscler Thromb*. 2011;18(9):796–807. doi:10.5551/jat.6569
66. Zhang X, Chen S, Yin G, et al. The Role of JAK/STAT Signaling Pathway and Its Downstream Influencing Factors in the Treatment of Atherosclerosis. *J Cardiovasc Pharmacol Ther*. 2024;29:10742484241248046. doi:10.1177/10742484241248046